1967

Velocity profiles in viscoelastic drag reducing solutions

Luis Gustavo Florez E.

Department:

VELOCITY PROFILES IN VISCOELASTIC DRAG REDUCING SOLUTIONS

BY

LUIS GUSTAVO FLOREZ E. - 1941

A

THESIS

submitted to the faculty of the

UNIVERSITY OF MISSOURI AT ROLLA

in partial fulfillment of the requirements for the

Degree of

MASTER OF SCIENCE IN CHEMICAL ENGINEERING

Rolla, Missouri

1967

Approved by

Jerry K. Tollerson (Advisor)

Jacques L. Zakin

Robert L. Davis

TABLE OF CONTENTS

Page

LIST OF FIGURES

Page

Page

LIST OF TABLES

Page

I ABSTRACT

Turbulent velocity profiles in viscoelastic drag reducing solutions were measured using hot-film anemometer and Pitot tube techniques. Data were obtained in a solution of one per cent aluminium dioleate in toluene and in 0.2 and 0.4 per cent solutions of polyisobutylene (PIB) L-200 in cyclohexane. Velocity profiles were also obtained for comparison in toluene and cyclohexane by both techniques.

By integrating the Pitot tube velocity profiles, large flow rate discrepancies between integrated and measured flow rates were found for the drag reducing polymer and soap solutions. This discrepancy was not observed in the hot-film anemometer measurements.

The hot-film anemometer results indicated flatter profiles for the drag reducing soap solutions and steeper profiles for the drag reducing polymer solutions compared with the solvents. A plot of the anemometer data at the highest Reynolds numbers in the form of u^+ versus log y^+ indicated an increase of thickness in the boundary layer for both soap and polymer solutions.

ACKNOWLEDGMENTS

The author wishes to extend his deepest appreciation to Dr. Gary K. Patterson for his assistance, inspiration, and encouragement throughout this investigation.

He also wishes to thank Dr. Jacques L. Zakin for his comments and patience in reading the present work, and Mr. Jorge M. Rodriguez, who spent long hours assisting the author in taking some of the velocity profile measurements.

He is grateful to "ICETEX," (Colombian Institute for Foreign Studies), for their support, which made graduate school financially possible.

Finally he is indebted to his parents for their constant encouragement.

II INTRODUCTION

Drag reduction in turbulent flow, which is a decrease in the pressure drop of a solution compared with its solvent under the same flow conditions, has been observed in certain types of fluids such as polymers and soap solutions. Measurements of normal stresses (i.e., through capillary jet-thrust techniques) have given evidence of viscoelasticity in these solutions.

Several theories have been offered using viscoelastic mechanisms to explain drag reduction. It is believed that a complete understanding of drag reduction phenomena requires a knowledge of the velocity profiles under drag reducing flow conditions. Investigators attempting to measure velocity profiles in viscoelastic solutions using Pitot tubes have generally observed discrepancies between flow rates obtained by profile integration and measured by weighing.

Therefore, this work was an attempt to measure quantitative velocity profiles of viscoelastic drag reducing solutions with two different velocity sensors: a Pitot tube and a hot-film anemometer.

III LITERATURE REVIEW

VELOCITY PROFILES IN PIPE FLOW OF NEWTONIAN FLUIDS

The substitution of Newton's law of viscosity for the shear stress in a shell momentum balance in laminar flow gives the expression describing the velocity profile in a round tube (2, 18), which in terms of the maximum velocity ocurring at the center of the tube is:

$$\frac{\bar{u}}{\bar{u}_{max}} = \left[1 - \left(\frac{r}{R}\right)^2\right] \qquad (1)$$

In the laminar regime, as observed by Reynolds (34) using dye injection techniques, the flow is composed of straight streamlines. However, if the Reynolds number is increased these streamlines become sinuous or turbulent for values of N_{Re} above 2100. In this turbulent region eddy formation occurs causing higher shear stress for a given velocity gradient as well as higher heat and mass transfer rates than for the laminar stream motion. References (17) and (27) discuss the turbulent motion mechanism and some modern theories and developments.

As the first step in obtaining an equation for the velocity profile in the turbulent regime, the Reynolds equations of motion for incompressible fluids are derived (17), based on the Navier-Stokes equation for constant viscosity. The Reynolds equations contain extra terms (Reynolds stresses) which are responsible for the greater shear stresses during turbulent flow. Solution of these equations for turbulent flow would

adequately describe the time averaged properties of the turbulent flow if the number of equations were equal to the number of unknowns. However, with the continuity equation there are only four equations present for ten unknowns. In order to obtain more specific results the following semi-empirical expressions have been suggested for the Reynolds stresses:

a) Boussinesq's Eddy Viscosity Expression (2), which is analogous to Newton's law of viscosity:

$$\bar{\tau}_{yx}^{(t)} = -\mu^{(t)} \frac{d\bar{u}_x}{dy} \qquad (2)$$

where $\bar{\tau}_{yx}^{(t)}$ is the turbulent (Reynolds) stress in the x direction on the surface of an element of fluid and $\mu^{(t)}$ is the turbulent coefficient of viscosity or eddy viscosity which depends on radial position. The total stress along the rz direction in pipe flow, is the sum of two contributions as follows:

$$\bar{\tau}_{rx} = -\mu \frac{d\bar{u}_x}{dr} - \mu^{(t)} \frac{d\bar{u}_x}{dr} \qquad (3)$$

where the first part of the right hand side of the equation describes the laminar contribution and the second part the turbulent one. Without an assumption of the variation of $\mu^{(t)}$ with position this concept cannot yield a velocity profile equation. Since little progress has been made in that direction, it will not be considered further.

b) Von Karman Similarity Hypothesis (38), which is based on dimensional analysis considerations:

$$\bar{\tau}_{yx}^{(t)} = -\rho k_k \left| \frac{(d\bar{u}_x/dy)^3}{(d^2\bar{u}_x/dy^2)^2} \right| \frac{d\bar{u}_x}{dy} \qquad (4)$$

in which the values of k_k (universal constant), are determined from experimental data.

c) Prandtl's Mixing Length Theory (42), which is based on an analogy of the eddy movement with molecular movement and includes a length parameter, l, proportional to the distance from the tube wall:

$$\bar{\tau}_{yx}^{(t)} = \rho l^2 \left(\frac{d\bar{u}_x}{dy} \right)^2 \qquad (5)$$

VON KARMAN VELOCITY PROFILE

Substitution of equation (4) into a shell momentum balance yields the von Karman expression for the velocity profile, which has the form:

$$\bar{u} = \bar{u}_{max} + \frac{u^*}{k_k} \left(\ln(1-\sqrt{1-y/R}) + \sqrt{1-y/R} \right) \qquad (6)$$

in which k_k is 0.40 by experiment, y is the distance from the wall, R is the pipe radius, and u* is the friction velocity. A recent improvement in the von Karman velocity profile is based on the addition of a constant. This equation,

$$\bar{u} = \bar{u}_{max} + \frac{u^*}{k_k} \left(\ln(1-\sqrt{1-y/R}) + \sqrt{1-y/R} \right) + b, \qquad (7)$$

well with experimental data in the region $0<r/R<0.85$

convi nient for comparison with new velocity data, i.e.

for non-Newtonian fluids. Goldstein (12) recommends a value of 0.295 for k_k and 0.172 for b, based on Nikuradse's (26) velocity profile data which has been accepted as some of the best available.

LOGARITHMIC VELOCITY PROFILE LAW

The Prandtl mixing length theory leads to a velocity profile equation of the form:

$$\bar{u} = \bar{u}_{max} - \frac{u^*}{k_p}\left(\ln\frac{1+\sqrt{r/R}}{1-\sqrt{r/R}} - 2\sqrt{r/R}\right) \tag{8}$$

where k_p is 0.4 by experiment and R is the pipe radius. This equation does not agree very well with experimental data. Better agreement is obtained by using the assumption:

$$\tau_{rx} \simeq \tau_w\left(\frac{r}{R}\right) = \tau_w \tag{9}$$

which is only valid in the region near the wall. With this assumption equation (8) becomes:

$$\bar{u} = \bar{u}_{max} + \frac{u^*}{k_p}\ln\left(\frac{R-r}{R}\right) \tag{10}$$

This equation fits experimental data fairly well in the region $0<r/R<0.85$, but not as well as the von Karman equation (38). Neither equation gives a zero slope at the pipe center.

Wang (48) has developed another expression for the velocity distribution, based on the mixing length theory. Experimental data is fit better by Wang's equation than by the logarithmic velocity profile equation; however, its complexity has made

it less useful. Another variation of the mixing length approach has been used by Gill and Scher (13) to derive a complex expression which reduces to equation 1 at N_{Re} = 1800. Their equation also gives a zero slope at the pipe center, but like Wang's equation, it is difficult to use.

UNIVERSAL VELOCITY PROFILE EQUATION

The Prandtl logarithmic velocity profile equation is generally used as the basis for the derivation of the universal velocity profile (UVP) equation, which is the most popular expression for turbulent velocity profiles and is also called the "law of the wall." In region near the wall turbulent and laminar flow coexist (18). Assuming a distance from the wall at which only turbulent flow exists and a viscous (nearly laminar) region at the wall, the intersection of the viscous (laminar) profile and turbulent profile at this distance gives:

$$u^+ = A + B \ln y^+ \qquad (11)$$

where $u^+ = \bar{u}/u^*$; $y^+ = u^* y/\gamma$

A = 5.5 and B = 2.5 by best fit to experimental data. The term y^+ is a modified Reynolds number, which is a function of the friction velocity, u^*.

The UVP equation fits experimental velocity profile data near the wall in the fully turbulent region. Ross (38) has recommended that it be used only for $y/R<0.15$ and for $y^+>20$. It does not account for the so called "wake" region near the

center of the pipe. This was shown by the data of Bogue (4), Nikuradse (26), Deissler (7), Hershey (15), Bunch (5), and Tao (45).

Local velocities measured by Deissler (7) for the flow of air in a smooth circular tube were fit better by the UVP equation, equation 11, when the value of A was set at 3.8 and B at 2.78. Actually, Deissler's data differ very little from the Nikuradse data when directly compared.

IMPROVEMENTS IN THE UNIVERSAL VELOCITY PROFILE EQUATION

The main problem in describing the velocity profile is the existence of the laminar, transition and turbulent regions and the difficulty in representing them by just one equation. Aware of this fact, Deissler proposed an empirical expression for use in the region near the wall. In this region he neglected the effect of the kinematic viscosity and found that this does not introduce serious error since the effect of this physical property is slight. His equation, given in reference (18), has the advantage that it represents in a single curve the profile for the laminar and transition regions, but is too long to reproduce here.

Another form of the UVP equation has been established by Millikan, Reichardt and Hinze (17), and Bogue and Metzner (4), to improve that equation. Their equation is of the form:

$$u^+ - C = A + B \log y^+ \qquad (12)$$

This equation only differs in the value of the constants A and B recommended and in the variable correction term C, which is a function of y/R for Millikan, Reichardt, and Hinze and a function of the friction factor as well as y/R for Bogue and Metzner. The term C forces a better fit to the data in the wake region at the pipe center.

NON - NEWTONIAN TUBE FLOW

The characterization of a fluid is accomplished by a study of the wall shear stress of the fluid as a function of the shear rate, and may be represented for laminar flow by the equation:

$$\tau_w = \frac{D\Delta P}{4L} = K'\left(\frac{8U}{D}\right)^{n'} \qquad (13)$$

In this equation, K' and n' are rheological parameters. Equation 13, the Rabinowitsch (31) and Mooney (25) relationship, supposes no slip at the wall and purely viscous behavior. When n' equals 1, the equation represents Newtonian fluids and values different from unity are an indication of how far a fluid is from Newtonian behavior.

Clearly, friction factors for turbulent flow of non-Newtonian fluids cannot be obtained from the von Karman friction factor equation because a constant viscosity term cannot be used. Thus, modifications of the expressions for the Reynolds number and friction factors have been proposed, of which the most popular is the Dodge and Metzner equation (9):

$$1/f = \frac{4.0}{(n')^{.75}} \log \left[N'_{Re} \, (f)^{1-n'/2} \right] - 0.40(n')^{1.2} \qquad (14)$$

$$\text{where } N'_{Re} = \frac{8U^2\rho}{g_c K' \left(\frac{8U}{D}\right)^{n'}} \qquad (15)$$

Equation 14 reduces to the von Karman equation for turbulent flow when n' equals one. Polymer solutions, soap solutions, and suspensions are examples of non-Newtonian fluids whose friction factors may be represented by equation 14, if they are purely viscous.

DRAG REDUCING TURBULENT TUBE FLOW

Reduced pressure drops for the turbulent flow of polymer solutions compared with the solvent at the same flow rate were observed by Toms (46) for low concentration solutions of polymethyl methacrylate in monochlorobenzene. Pressure drop values as much as 50 per cent below the solvent at the same flow rate were noticed.

The effect observed by Toms has been called drag reduction (39). In terms of pressure drop the following concepts are used:

DRAG RATIO (15, 16): The ratio of the pressure drop for the solution to the observed pressure drop of the solvent at the same flow rate.

FRICTION FACTOR RATIO (28, 35, 36): The ratio of the measured

friction factor to the friction factor predicted by equation 14, at the same Reynolds number.

A thorough review of drag reduction has recently been made by Patterson, Zakin, and Rodriguez (30).

TURBULENT VELOCITY PROFILES IN DRAG REDUCING POLYMER SOLUTIONS

Most of the hypotheses which attempt to explain drag reduction in the turbulent flow of polymer solutions depend on the viscoelasticity of the polymer molecules (3, 9, 16, 41, 49). Viscoelasticity has been confirmed for the more concentrated drag reducing solutions by the measurement of finite normal stress differences in the solution. Characteristic relaxation times calculated from molecular theory have been used to correlate drag reduction with flow rate in pipe flow. References (9), (15), (30), (35), and (36) discuss this topic in some detail. Patterson (28, 29) proposed a mechanism which demonstrates the relative effects of viscoelasticity and viscosity on drag reduction, and Rodriguez, Zakin, and Patterson (36), through a dimensional analysis approach, determined a relation for the reduction of friction factor below the purely viscous friction factor of Dodge and Metzner, equation 14, resulting in a complex and more general representation of drag reduction in viscoelastic flow.

Almost all the measurements of velocity profiles in drag reducing fluids have been made with impact tubes which measure

the fluid's velocity head. In 1957 Shaver (43, 44) measured turbulent velocity profiles of solutions of carboxymethyl cellulose (CMC) whose non-Newtonian behavior corresponded to $0.54 \leq n' \leq 1.0$. He plotted velocity deficiency against the dimensionless group y/R. The conclusion he drew from his work was that the velocity profiles became steeper for more pseudoplastic fluids. This was actually not true if his profiles were plotted as $\bar{u}/\bar{u}_{max}$ versus y/R (15), but gave that appearance since he was plotting a velocity deficiency divided by u*, and u* decreased as n' decreased since the solutions became more drag reducing.

Hershey (15) integrated all of Shaver's profiles to obtain the bulk mean velocity in order to check the material balance. The result was that integrated velocity profiles averaged six per cent below measured flow rates. Hershey also concluded that the presence or absence of slip at the wall cannot be decided from Shaver's data.

Bogue (3) attributed the anomalies of Shaver's profiles to viscoelastic effects in the drag reducing CMC solutions. Bogue measured velocity profiles of water solutions of Carbopol and Attagel (both non-drag reducing) in two different tube sizes and plotted his results as velocity deficiency against y/R. He concluded that no appreciable differences were observed when his profiles were compared with Newtonian profiles. It is important to point out that for the dilute solutions in this discussion no difference between solution and solvent density is noticeable, so that for a given solvent-solution system the-

only physical properties that are changed by solute addition are the viscosity and the elastic modulus.

Clapp (6) measured velocity profiles in dilute non-drag reducing solutions of Carbopol. They were replotted by Eissenberg (10) who concluded that no appreciable difference from Newtonian profiles could be discerned. The same conclusion is reached when studying Eissenberg's solid suspension profiles, although a small trend to steeper gradients is noticeable.

Ernst (12) measured velocity profiles in drag reducing CMC solutions, and he plotted his results as u^+ versus ln y^+ based on wall viscosity, and found higher u^+ values compared with Newtonian fluids. His integrated profiles, however, average seven per cent lower than his measured average velocities.

Wells (49) measured velocity profiles for CMC solutions and guar gum solutions. He noticed the same upward shift that Ernst noticed plus an increase in the slope of u^+ versus ln y^+. His profiles average six per cent low when compared with measured flow rates. Hershey (15), plotted Well's profiles and found that they were more blunt when they were plotted as dimensionless velocity ($\bar{u}/\bar{u}_{max}$) versus dimensionless position (y/R). The bluntness of Wells' velocity profiles in comparison with Newtonian profiles have led some investigators to explain drag reduction by a mechanism involving slip at the wall. However, as Patterson (28) points out, this observation does not necessarily indicate slip at the wall. Based on zero wall velocity, an infinite number of profiles are possible. For this reason

determination of the absence or presence of slip at the wall by measuring the profiles of drag reducing solutions away from the wall and comparing them with Newtonian profiles to determine whether or not the former are blunter is not valid.

The latest work to be interpreted as evidence of slip at the wall was done by Virk (47). He measured friction factors and velocity profiles for the turbulent flow of five homologous polyethylene oxides with water as the solvent. The flow rates obtained by integration of Virk's polymer velocity profiles are below the corresponding measurements in water. He observed that Pitot tube size affected his local velocity measurements. The discrepancy between integrated and calibrated flow rates diminished with increased Pitot tube size and with decreasing flow rate for a given Pitot tube size. He therefore used a larger Pitot tube for high flow rate measurements.

The conclusion drawn from his data is that local velocities taken with impact tubes are functions of the Pitot tube size, the molecular weight, and the concentration of the polymer solution, and that blunter profiles prevail when drag reduction is present, which as said before motivated his slip model explanation. It should be noted that velocities sufficiently near the wall have not been taken, by Virk nor by any other investigator, to eliminate the uncertainty of extrapolating profiles to the tube wall. Virk's data are also consistent with the explanation of drag reduction based on viscoelasticity.

Elata (11), using the viscoelastic model behavior of the

polymer molecules, made a direct correction to the velocity distribution expression by taking into account the ratio, relaxation time / flow time (Deborah number (22, 33)), in the form:

$$\frac{u^{*2}\tau_1}{\nu}$$

In this way he obtained a new law of the wall equation:

$$\frac{\bar{u}}{u^*} = \frac{1}{k} \ln\left(\frac{yu^*}{\nu}\right) + 5.5 + \alpha \ln\left(\frac{u^{*2}\tau_1}{\nu}\right) \qquad (16)$$

where the Deborah number was obtained empirically and α is a polymer characterization constant. τ_1 is the first mode relaxation time for the polymer in solution given by the Rouse theory. A test of this equation was accomplished by Elata by extending it to obtain an expression for friction factor, which resulted in good agreement with his data for guar gum in water with α evaluated empirically at a given concentration.

VISCOELASTIC EFFECTS ASSOCIATED WITH VELOCITY PROFILE MEASUREMENTS

In the majority of the studies accomplished up to this time, the Pitot tube has been taken as the true velocity transducer for velocity profile experiments. In turbulent flow, the expression holding for the measurement of the local velocity is given by:

$$P_i = \frac{\rho \bar{u}_x^2}{2g_c} \qquad (17)$$

where P_i is the impact pressure, ρ is the fluid density, and $\tilde{u}_x$ is the local velocity of the fluid at a given position. However, Astarita (1) has shown, assuming no area for the

Pitot tip and no alteration of the flow by the presence of the Pitot tube, that the time averaged values indicated by a Pitot tube are given by,

$$P_p = -\bar{\sigma}_x + \frac{\rho \bar{u}_x^2}{2} \tag{18}$$

where $-\bar{\sigma}_x$ is the time averaged value of the normal stress in the direction of flow.

The pressure reading at the wall at the same axial position is:

$$P_w = -(\sigma r)_{r = R} = -(\bar{\sigma} r)_{r = R} \tag{19}$$

A differential momentum balance in the radial direction gives the correct expression for the differential Pitot tube pressure readings as follows:

$$P_p - P_w = \underbrace{-(\bar{\sigma}^\circ_x - \bar{\sigma}^\circ_r)}_{A} \underbrace{- \int_r^R (\bar{\sigma}^\circ_r - \bar{\sigma}^\circ_\theta)\, d \ln r}_{B} \underbrace{+ \frac{\rho \bar{u}_x^2}{2}}_{C} \tag{20}$$

where terms A and B correspond to the first normal and integral normal stress differences, respectively, and term C is the velocity head component of the differential reading. For the turbulent flow of purely viscous fluids, equation 20 reduces to the usual expression for Pitot tube measurements-term C.

Thus, terms A and B form the elastic contribution to the Pitot tube measurement and are functions of the radial position. Term A represents the finite normal stress contribution which has its maximum value at the tube wall and is zero at the center of the tube where term B or the integral normal stress contribution

is finite. On the other hand, the velocity head component, term C, has its maximum value at the center of the tube and should be zero at the tube wall.

Solving for velocity in the usual expression for Pitot tube readings as

$$\bar{u}_x = \sqrt{\frac{2\Delta P_{gc}}{\rho}} \tag{21}$$

gives values of this quantity which are masked by the normal stress components of equation 20. Furthermore, the signs of the normal stresses in this equation are negative, so the apparent values of velocity will appear lower in a velocity profile study and the profile will be distorted, if no evaluation of terms A and B is made.

Savins (39) has proposed a method for evaluating first normal stress differences in laminar flow conditions using the deviations from expected values for Pitot tube measurements.

Astarita (1) measured velocity profiles of viscoelastic solutions of ET597* in water and his integrated flow rates were below the flow rates measured directly. He concluded that the elastic effects in the central region of the tube, from Pitot tube measurements, are much larger than at the wall in contrast with the laminar flow case.

---

*Dow Chemical Company

In conclusion, the following statements can be made based on the present data available for velocity profiles in the turbulent flow of viscoelastic drag reducing solutions:

a) It is not possible to get an exact check of directly measured bulk flow rates of viscoelastic fluids with flow rates calculated by integration of point velocities measured by Pitot tube techniques. The integrated profiles always yield flow rates which are less than the true bulk flow rates for such fluids.

b) The local velocities indicated by Pitot tube velocity profile measurements indicate distortions of the velocity distributions, because they include normal stress effects caused by the viscoelasticity of the solutions.

c) Blunter profiles are observed in the Pitot tube velocity profile measurements in viscoelastic solutions compared with profiles for the Newtonian solvent, but this effect might be caused by the distortion mentioned above.

Therefore, there is a need to develop a technique to measure velocity profiles in viscoelastic systems. Part of this investigation was a study of the use of a hot-film anemometer sensor for this purpose.

IV EXPERIMENTAL

The main purpose of the experimental part of the present investigation was the measurement of velocity profiles in the turbulent flow of drag reducing fluids with a Pitot tube and and a hot-film anemometer in round smooth tubes.

MATERIALS

Toluene: Purity (wt % toluene) 99.5% minimum; impurities-heptane isomers 0.5% maximum; maximum boiling range 1°C, including 110.6°C. Specific gravity between 0.865 and 0.873 at 15.5°C. Nitration grade; purchased from G. S. Robins Co., St. Louis, Missouri.

Cyclohexane: Purity (wt % cyclohexane) 99.9% minimum; impurities non-volatiles, water, benzene 0.1% maximum; maximum boiling range 0.4°C, including 80.7°C; specific gravity 0.780-0.784 at 15.5°C. Purchased from G. S. Robins Co., St. Louis, Missouri.

Aluminium Soap: Thickener agent, prepared from fatty and organic acids plus additives. Essentially a dioleate of aluminium with a moisture content of 0.6% and a free fatty acid content of 6.1% (as oleic acid). Sample from Witco Chemical Company, Inc., Chicago, Illinois.

Polyisobutylene L-200: Enjay HM Vistanex; grade L-200; lot B31006; code 054; viscosity average molecular weight 4,000,000 -4,700,00, distribution unknown; exact production method and

catalyst content unknown; color, white; donated by Humble Oil and Refining Co., Baton Rouge, Louisiana.

APPARATUS

The local velocity measurements were made in a pipe flow unit provided with a test section with three carbon steel tubes, of which the one with a diameter of one inch was used. Reference (15) discusses in detail the variables in the design of the unit as well as the information concerning the construction. Figure 1 is a diagram of the unit, and the physical dimensions of the one inch tube test section are as follows:

Diameter:		0.999 inches
Length	:	200.0 inches
L/D	:	200

The fluid was pumped from a 100-gallon capacity reservoir through the test section and back into the reservoir. A Viking positive displacement pump, rated at 200 gallons per minute, was driven by a variable speed transmission which permitted a continuous variation of the flow rate. The flow rate was measured by turbine meters which produced a fluctuating voltage whose frequency was measured with a digital counter. Flow rates were measured after each set of profiles by diverting the flow to a weighing tank in order to establish the dependence between the frequency measurement and the flow rate through the test section. Surge volumes were located at the inlet manifold of

FIGURE 1. DIAGRAM OF THE PIPE FLOW UNIT

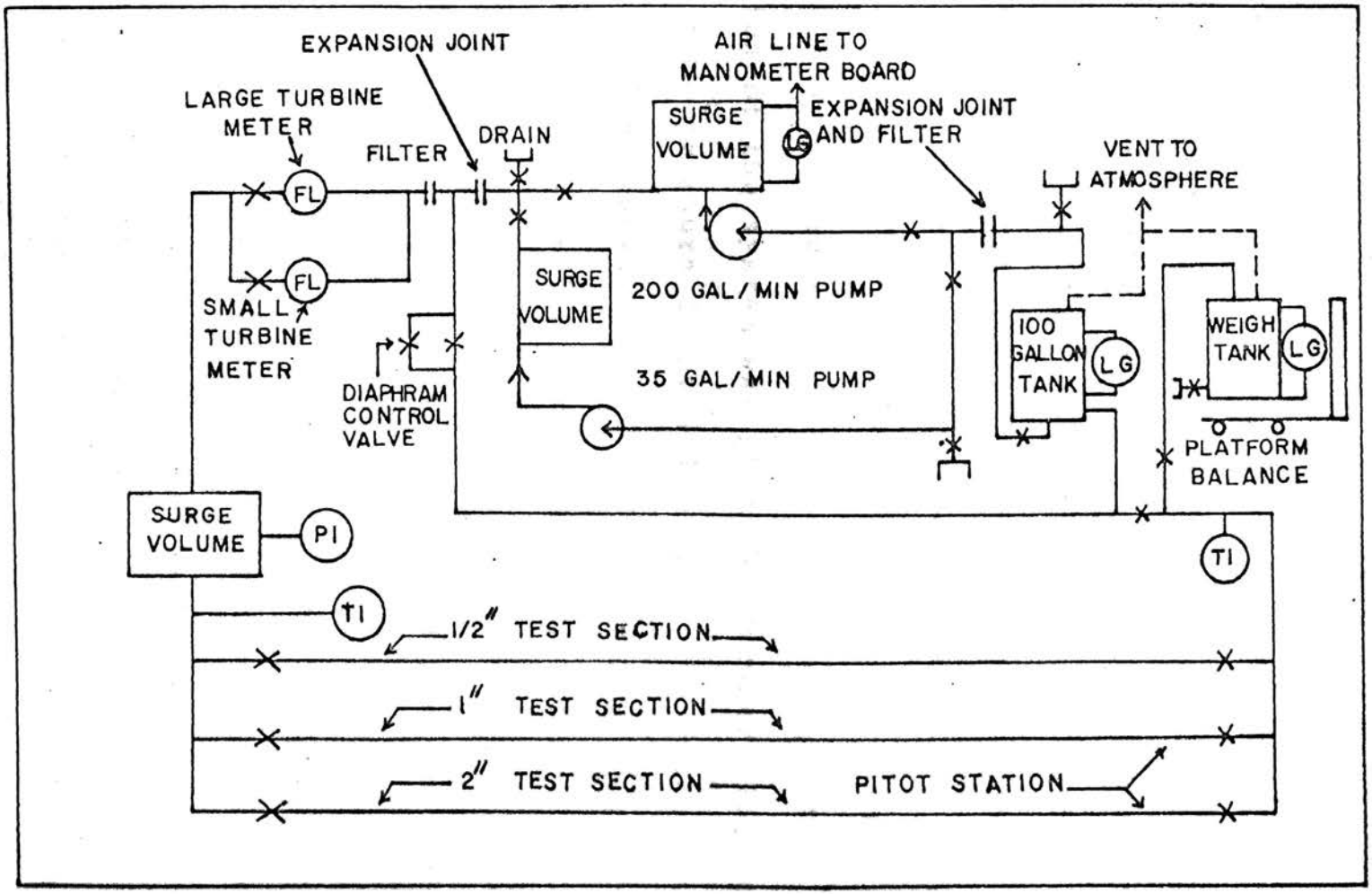
EXPANSION JOINT
AIR LINE TO MANOMETER BOARD
LARGE TURBINE METER
FILTER
DRAIN
SURGE VOLUME
LG
EXPANSION JOINT AND FILTER
VENT TO ATMOSPHERE
FL
FL
SMALL TURBINE METER
SURGE VOLUME
200 GAL/MIN PUMP
35 GAL/MIN PUMP
DIAPHRAM CONTROL VALVE
100 GALLON TANK
LG
WEIGH TANK
LG
PLATFORM BALANCE
SURGE VOLUME
PI
TI
TI
1/2" TEST SECTION
1" TEST SECTION
2" TEST SECTION
PITOT STATION

the test section to damp out disturbances, as well as in the pump discharge line. A by-pass line allowed the fluid to be pumped directly to the tank without passing it through the test section.

A filter made of 250 mesh Tyler sieve of about 72 square inches area removed small lint and dirt particles whose presence had a deleterious effect on the calibration of the hot-film anemometer by collecting on the heat transfer surface.

A sensitive temperature contol system was used, which held the temperature of the fluid within $\pm$ 0.02°C as required by the low overheat hot-film anemometer measurements. The operating temperature was set with a thermoregulator. A complete description of the system was given by Hershey (15, 16).

The tube pressure drops and velocity profiles with the impact tube were measured with two manometers (Fig. 2), which are described in detail in Reference (15). They were as follows:

a) A mercury U-tube manometer with fluid traps, 9 feet high.

b) An inverted U-tube manometer with process fluid as the indicator, 9 feet high.

These manometers were connected to an air regulator to control the position of the air-liquid interface. By selecting the proper valves on a valve table, the appropriate manometer was valved-in. The total pressure drop in the test section was read on one of the two manometers connected to the taps of the test section or impact tube by nylon tubing.

PITOT TUBE ASSEMBLY

A special impact probe was designed by Patterson (28) with an outside diameter of 0.036 inches at its tip. The tip was connected to the support tube by threads sealed with teflon. This Pitot tube was assembled in a probe mount designed by Hershey (15). Figures 3 and 4 show the Pitot tube and the probe mount for the one-inch tube test section. Nylon mounting bushings were used for the probe, which was installed in a one-inch machined cross with a one-inch inside diameter, providing a smooth wall behind the probe tip which minimized flow disturbances propagated upstream toward the probe tip.

The use of an electrical resistance method, using an ohmmeter allowed radial location of the impact tube by touching the wall to close a circuit. This established the reference position with an accuracy of $\pm$ 0.0005 inches. The probe was not allowed to contact the wall during measurements, so the reference wall position was only approached. The reference position was checked periodically after each profile measurement.

CONSTANT TEMPERATURE ANEMOMETER

Appendix I discusses briefly some theoretical aspects of anemometry and points out the principal characteristics of the method used.

The constant temperature anemometer used was a model 55A01, manufactured by DISA Electronik, Herlev, Denmark. The detailed specifications are shown in the DISA instruction

FIGURE 2. PHOTOGRAPH OF THE MANOMETERS

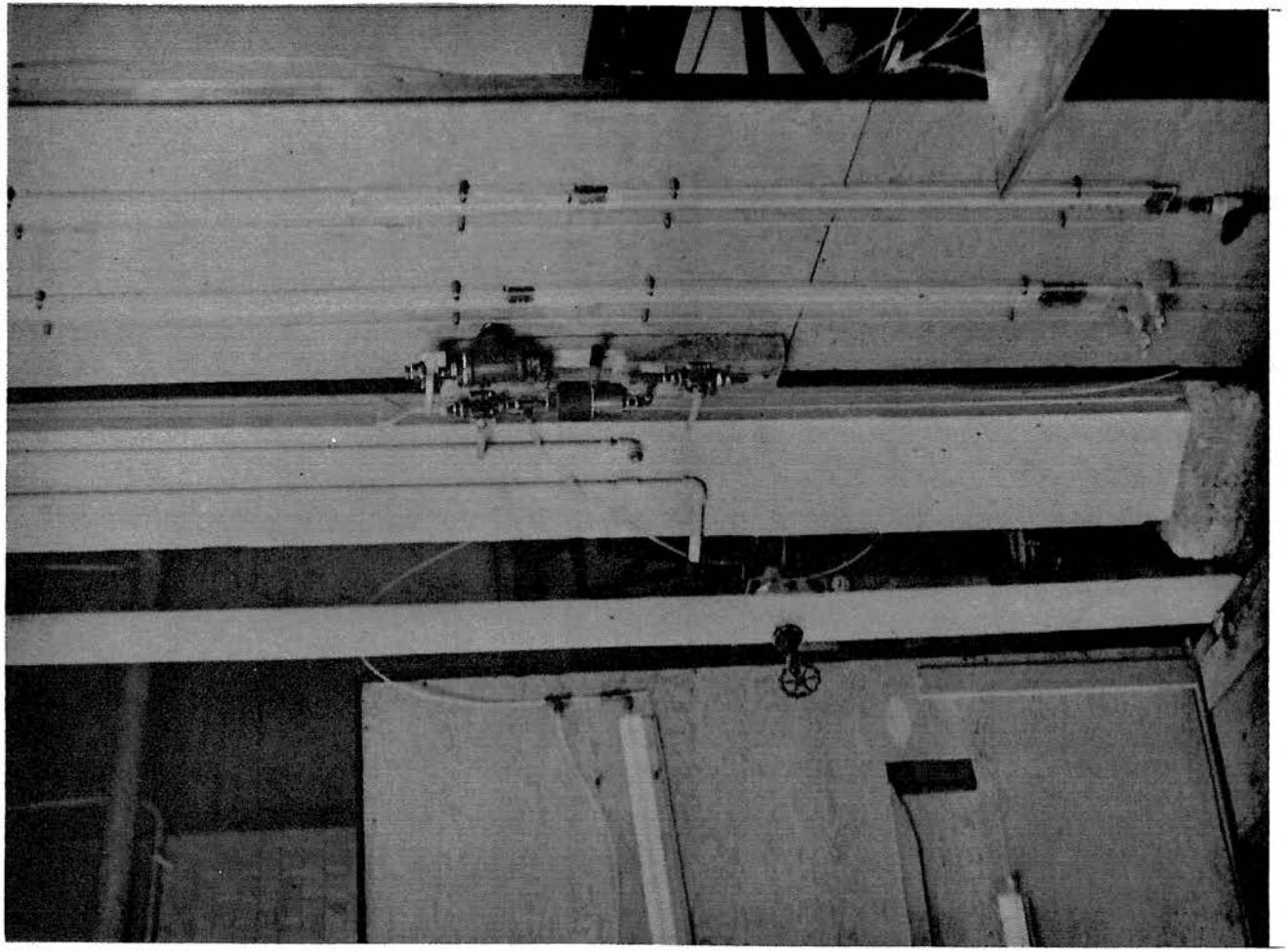

FIGURE 3. DIAGRAM OF THE PITOT TUBE

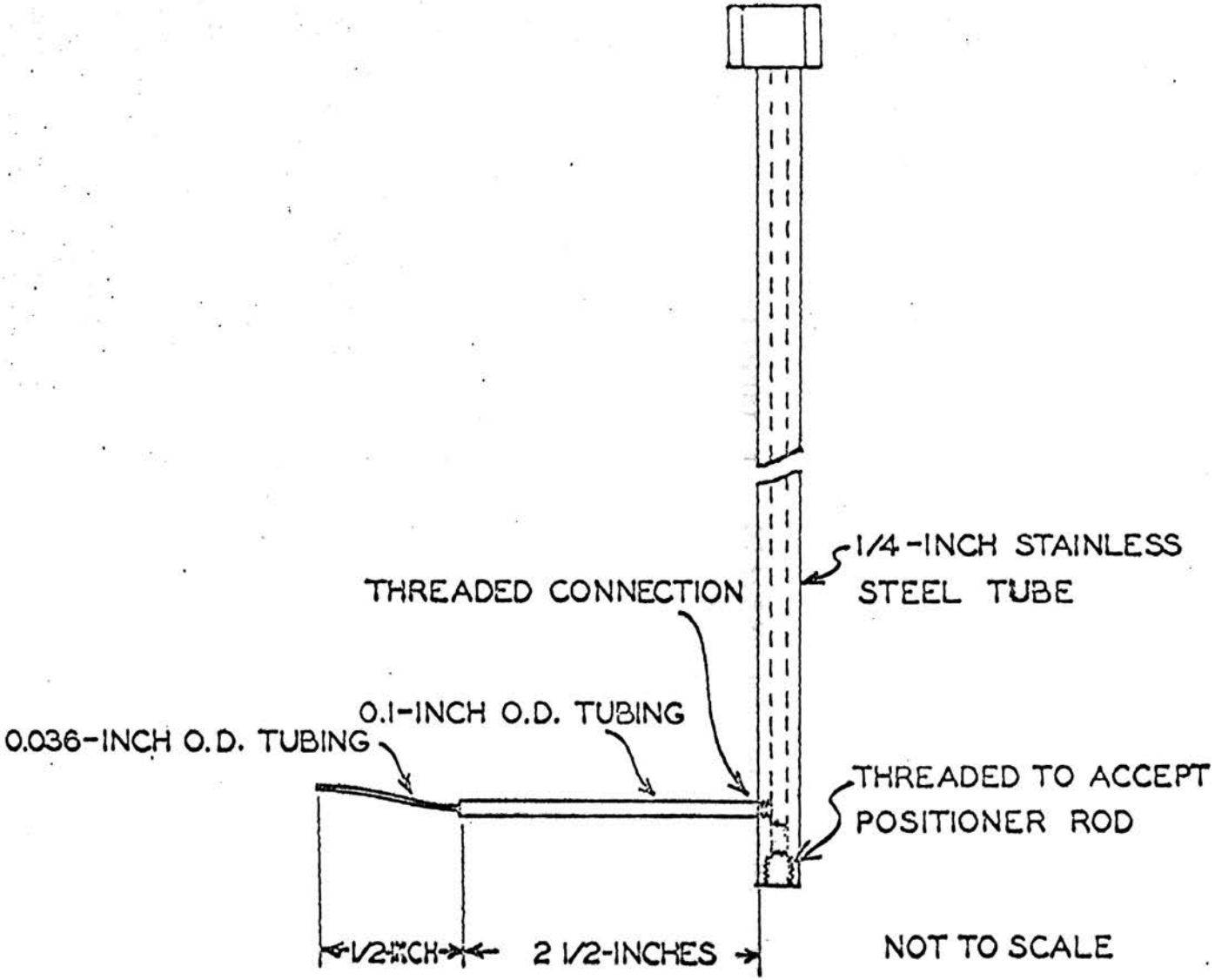
1/4-INCH STAINLESS
STEEL TUBE
THREADED CONNECTION
0.1-INCH O.D. TUBING
0.036-INCH O.D. TUBING
THREADED TO ACCEPT
POSITIONER ROD
1/2-INCH
2 1/2-INCHES
NOT TO SCALE

FIGURE 4. DIAGRAM OF THE PROBE MOUNT

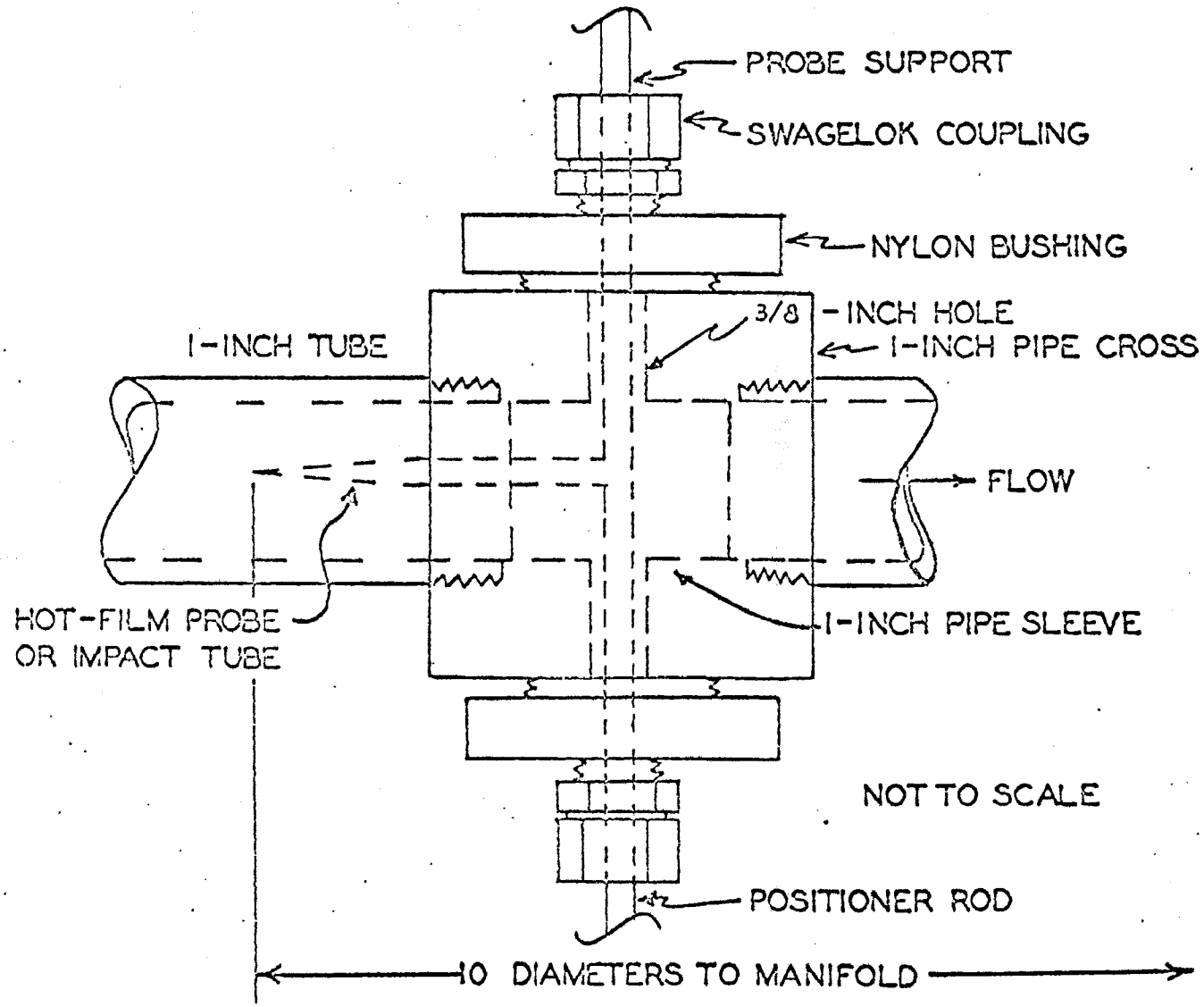
PROBE SUPPORT
SWAGELOK COUPLING
NYLON BUSHING
3/8 - INCH HOLE
1-INCH PIPE CROSS
1-INCH TUBE
FLOW
HOT-FILM PROBE
OR IMPACT TUBE
1-INCH PIPE SLEEVE
NOT TO SCALE
POSITIONER ROD
10 DIAMETERS TO MANIFOLD

manual (8). The major items are as follows:

Frequency response:	0-50 kcps.
Probe resistance range:	1-50 ohms.
Maximum probe current:	250 ma.
Amplifier transductance:	approximately 8 ma/mv at 125 ma current output.
Cold resistance measurement accuracy:	0.5%
Direct current voltmeter:	1% of full scale accuracy
Scales:	0-2, 0-5, 0-10, 0-20 volts with zero shift voltages of 1, 2, 5, and 10 volts.

The anemometer was equipped with a three decade balance resistor for measuring cold resistances to the nearest 0.01 ohm and for setting probe operating resistances.

Because of the importance of obtaining accurate values of DC voltages during the measurements, two additional pieces of equipment were used:

a) Time-Average Circuit: This part of the anemometer set-up was used in measuring the velocity profiles of the soap solution because of the large low frequency voltage fluctuations in the anemometer output. The instrument was basically an operational amplifier circuit whose input was the voltage from the hot-film manometer and whose output was a lag response with a gain of one indicated by a Digitec digital voltmeter. The circuit time constant was about three seconds.

b) Digital DC Voltmeter: This instrument was used for measuring DC voltages for velocity profiles in cyclohexane and in poly-isobutylene solutions. In these fluids the low frequency voltage fluctuations were of lower intensity than in the soap solutions, so the time averaging circuit was not necessary. The digital DC voltmeter was a model 55D30 manufactured by DISA Electronik, Herlev, Denmark, with ranges of 1, 10, and 100 volts, and a readout of 4 digits with automatic decimal point. Other characteristics are as follows:

Accuracy:	± 0.3% of range in use
Input Impedance:	1 megohm

HOT-FILM PROBE

The hot-film probe used was manufactured by Thermo-Systems Inc., Saint Paul, Minnesota, Model 1212-60. Dimensions of the film and general shape are shown in Fig. 5. This is a quartz coated hot-film cylindrical sensor with needle supports. Some other characteristics are as follows:

Relative frequency response:	15,000 cps at -3db, typical.
Sensor size:	0.006 inches dia. x 0.010 inches long.
Operating temperature:	up to 150°C.

The hot-film anemometer was installed in the tube test section using the same probe mount (Fig. 4) as was used in the impact tube measurements.

FIGURE 5 DIAGRAM OF THE HOT-FILM CYLINDER ANEMOMETER

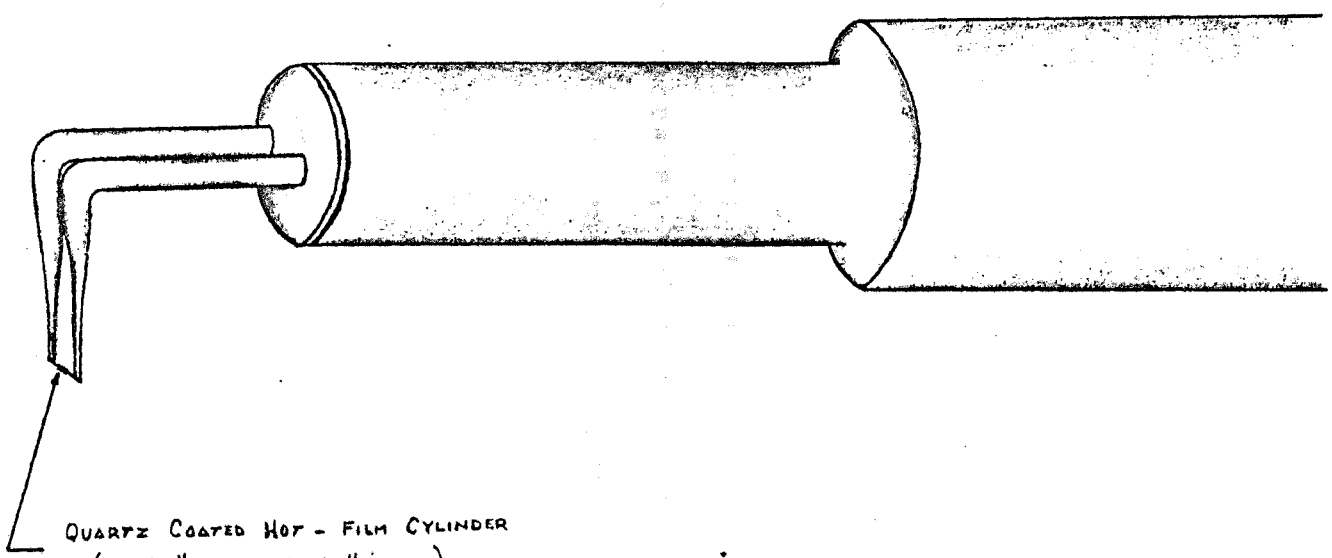
QUARTZ COATED HOT - FILM CYLINDER
(0.006" DIA. x 0.008" LONG)

EXPERIMENTAL PROCEDURE

The procedure used to take velocity profiles with impact tubes in the tube test section described was reported by Hershey (15). Only the principal steps will be given here, as well as a short description of the measurements of velocity profiles with the hot-film anemometer. Sample calculations are shown in Appendix II.

The preparation of the solutions was accomplished by using a Pyrex vessel equipped with a low speed air driven stirrer. These stock solutions were then mixed in adequate amounts to obtain the desired concentration in the flow system. The solutions were pumped for about two hours at low flow rates to disperse the concentrated solution uniformly in the solvent or solution already present in the system and to reach lower degradation rate conditions before making the measurements.

A flushing fluid was introduced in the unit between the measurements of velocity profiles for the soap solution and for the polymer solutions.

PITOT TUBE VELOCITY PROFILE MEASUREMENTS

In making the local velocity head pressure readings, the desired flow rate was established and the control temperature obtained. The wall position was obtained as described above with an ohmmeter. The "play" developed by the micrometer positioner as a consequence of wear was avoided by advancing the probe

only in the direction of the wall opposite to the support mechanism. Once the desired position within the tube was established, the proper manometer was valved-in and when equilibrium pressure was observed the reading was recorded after checking the temperature and the flow rate. The Pitot tube was then moved to a new position and the procedure repeated.

Frictional pressure drops, for determination of drag ratios, were measured after each profile. The flow rate was measured for each profile using the weigh tank described above.

HOT-FILM ANEMOMETER VELOCITY PROFILE MEASUREMENTS

The first step in the measurements with the hot-film anemometer was the location of the cylindrical film within the tube in order to establish the desired radial position of the probe during voltage readings. Thus, a position near the wall was determined using an optical technique with the aid of a telescope and a strong light source. The telescope was provided with a reticle scale so that the distance between the cylindrical film and its reflection on the smooth tube surface could be observed clearly. The micrometer positioner was moved so that the distance between the film and its reflection was reduced to one-half the original distance. The distance moved was one-half the original probe wall separation, so the true radial position could be obtained with an accuracy of $\pm$ 0.001".

In order to measure the velocity profile, the relation between the fluid velocity and the hot-film anemometer voltage must

established. Therefore, measurements of probe voltages at different flow rates were made at the tube axis, where the average velocity could be determined by methods described in the discussion of results. These values provided the necessary data to establish the calibration curve by determining the best least squares fit to the equation:

$$E^2 = A + B(\tilde{u})^C,$$

from which values of velocities could be determined by solving for $\tilde{u}$.

Calibration measurements were made before and after each profile in order to check consistency.

After locating radial probe positions, the probe resistance was established at fluid temperature and the desired operating resistance determined for a temperature well below the fluid boiling point. As far as the fluid heat transfer characteristics allowed, the operating resistance was kept at values greater than 1.05 times the cold resistance, since at these levels the small changes in temperature ($\pm$ 0.02°C), of the process fluid during velocity profile measurements did not influence the voltage readings.

The hot-film anemometer radial scanning was accomplished in the same way as with the Pitot tube, to determine local voltages and consequently local velocities. Careful fluid temperature control was necessary to obtain reliable experimental values. Checks of probe resistances at the fluid temperature were made after each set of profiles as well as

voltage readings at zero velocity. Pressure drops through the test section were measured after each profile to determine values of friction factors.

V DATA AND RESULTS

Since this investigation involved the measurement of velocity profiles with two different types of sensors, this section will treat the Pitot tube and the hot-film anemometer data separately.

PITOT TUBE VELOCITY PROFILES

A total of 20 profiles with the impact tube were taken, which are reported in Appendix III, Runs 1-20. Figures 6 - 15 show the velocity profiles for the solvent and solutions. The von Karman velocity distributions for the same solvent Reynolds numbers are shown as solid lines for comparison. The profiles are plotted as ($\bar{u}$/UAVGC) versus (y/R), where $\bar{u}$ is the local velocity and UAVGC is the average velocity measured by weighing. The latter has been chosen to normalize the local velocities because it does not mask effects that occur in some measurements in regions close to the tube axis.

Table I reports drag ratio values of the solutions--1.0 per cent aluminium dioleate in toluene, and 0.2 and 0.4 per cent PIB L-200 in cyclohexane. These values are calculated as the ratio of the friction factor of the solution to the friction factor of the solvent at the same flow rate, assuming negligible change in density upon addition of the solute.

TOLUENE-ALUMINIUM DIOLEATE SYSTEM

Figures 6-9 show Pitot tube velocity profiles for toluene

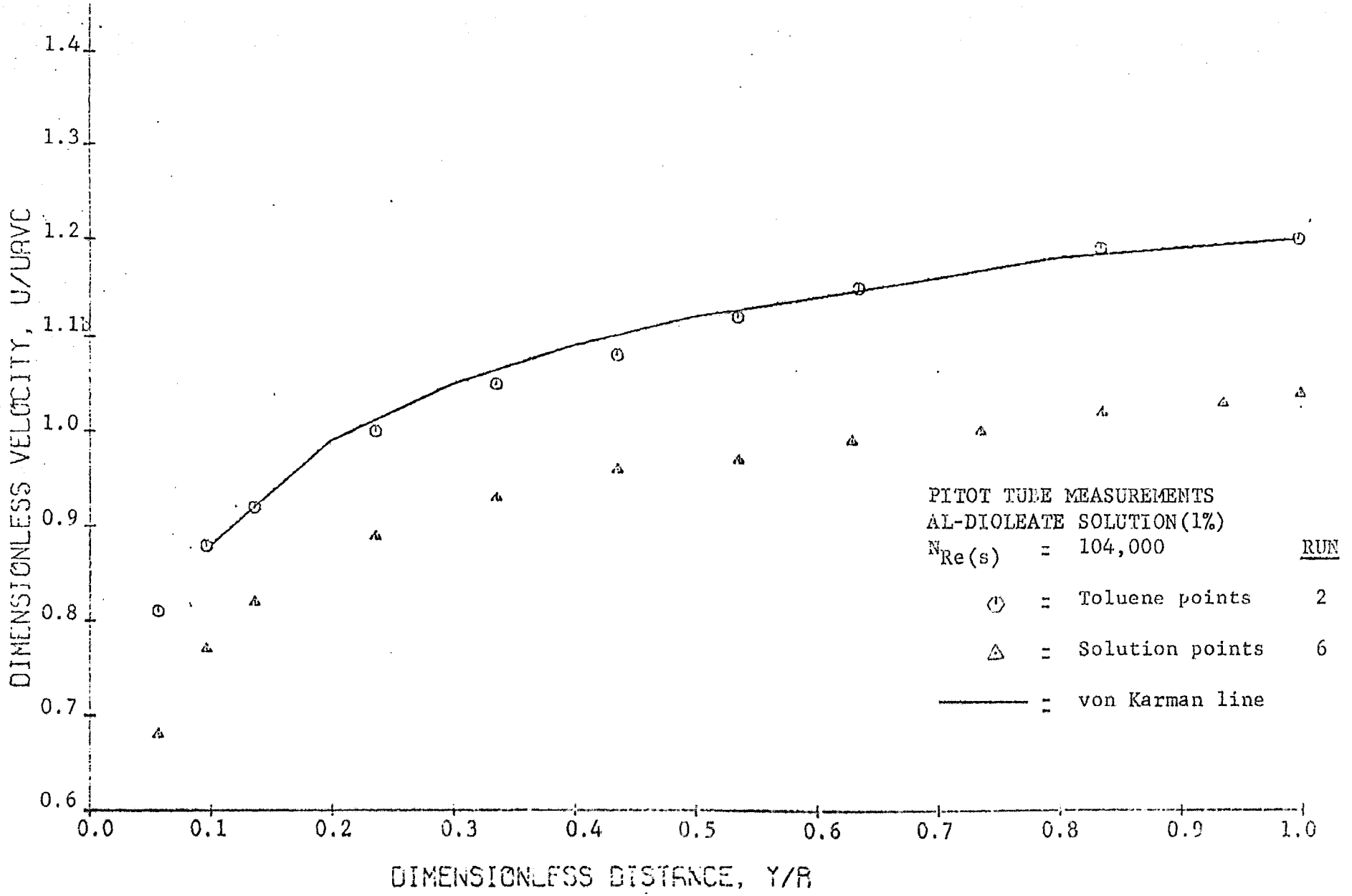

FIGURE 6
VELOCITY PROFILES

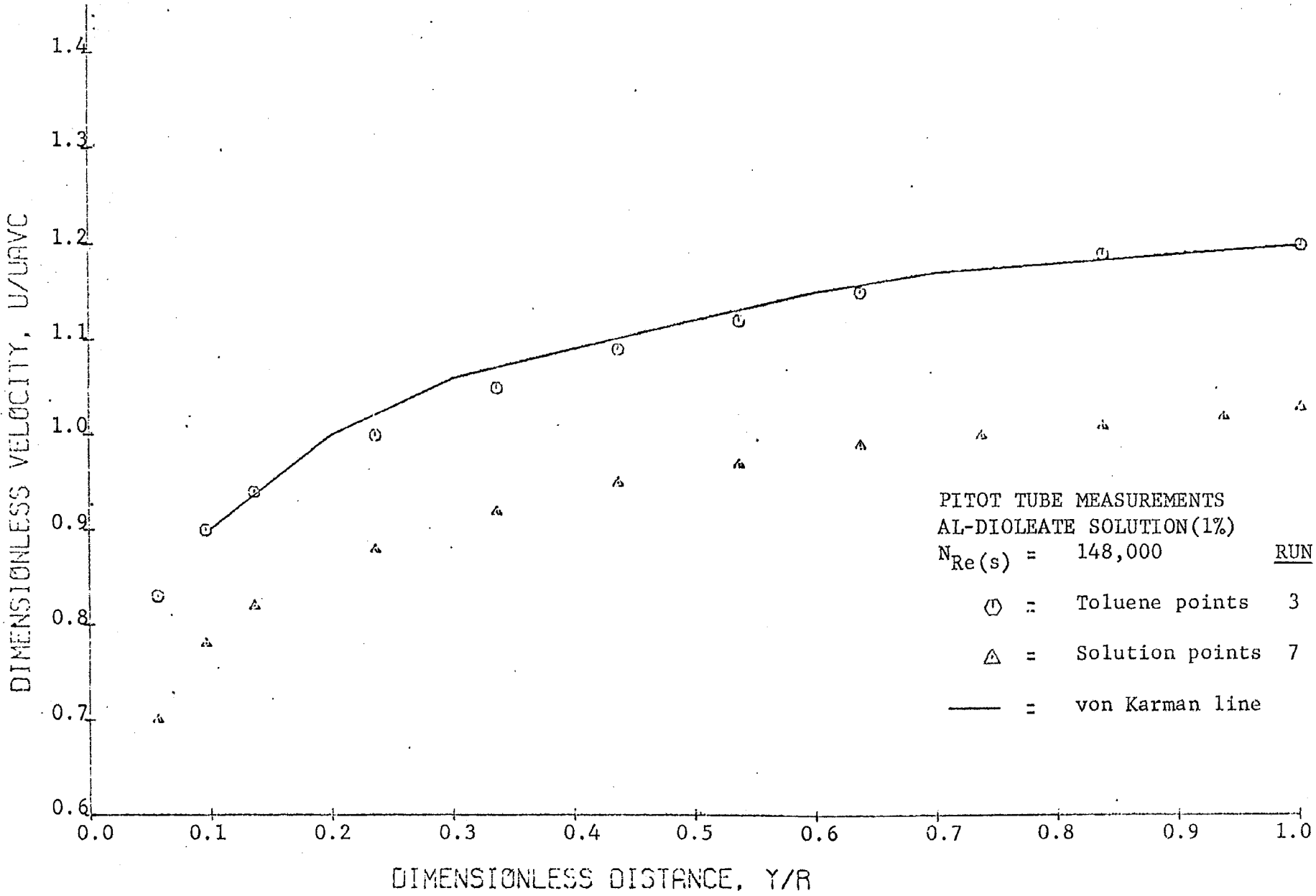

FIGURE 7
VELOCITY PROFILES

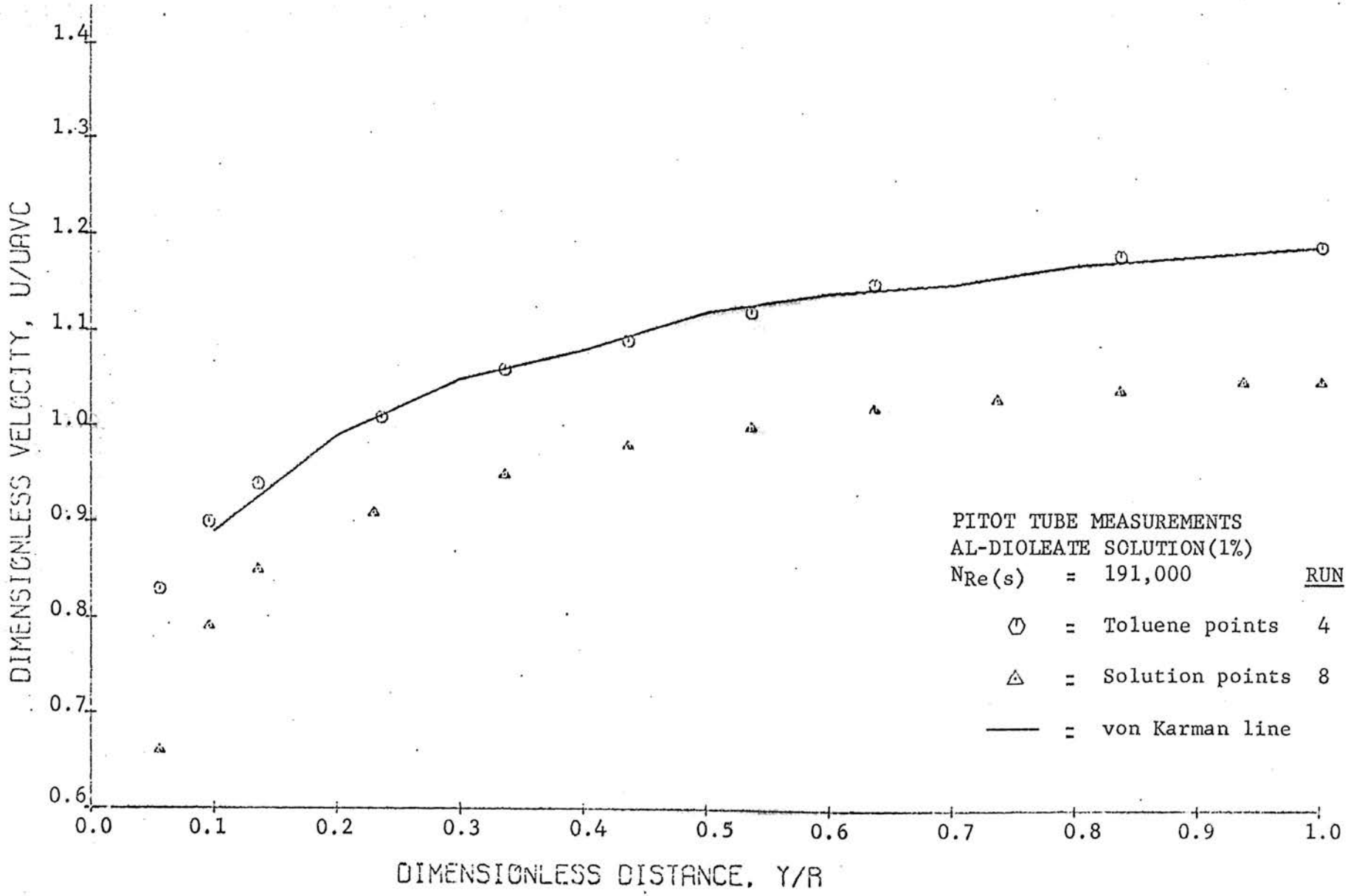

FIGURE 8
VELOCITY PROFILES

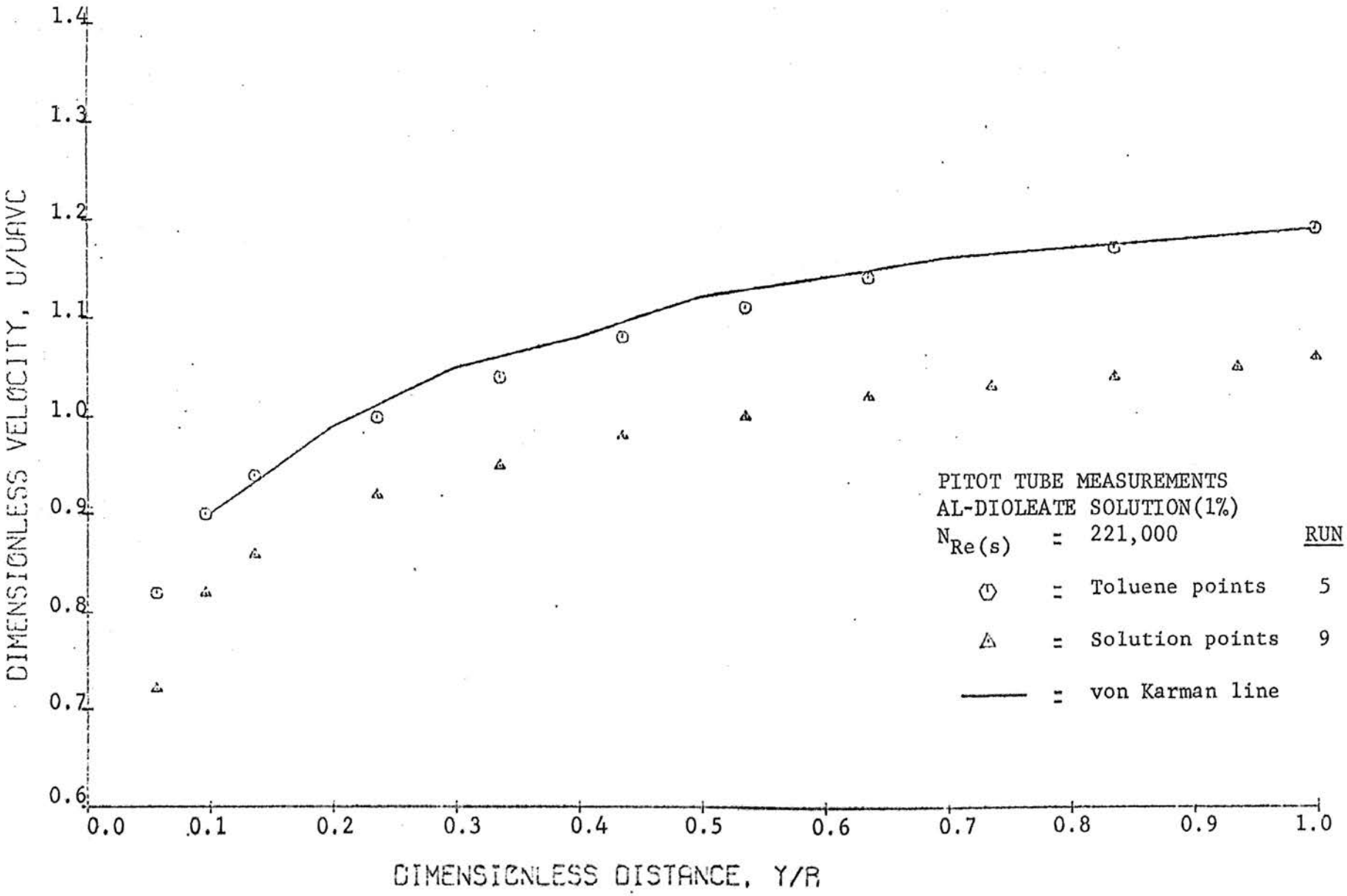

FIGURE 9
VELOCITY PROFILES

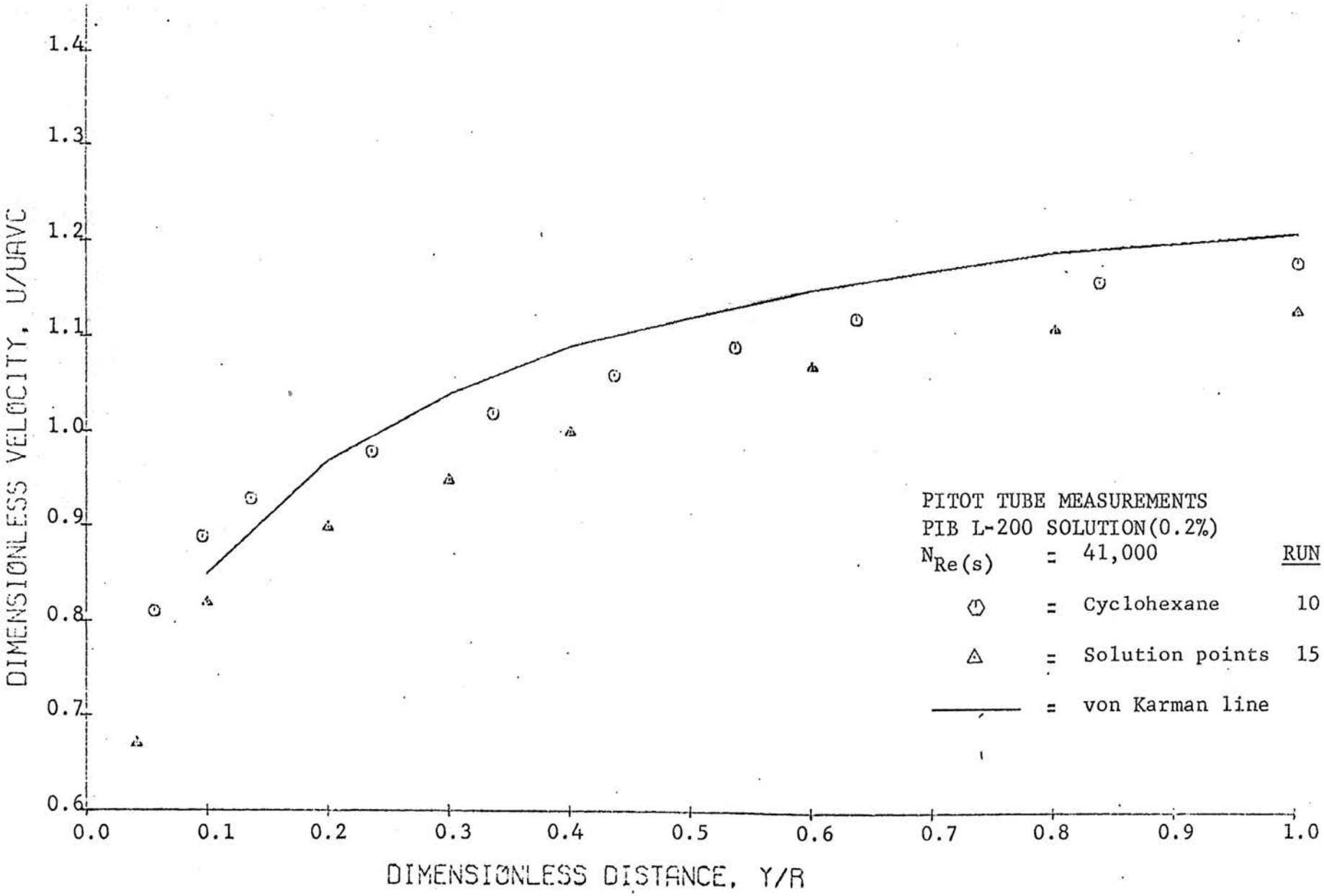

FIGURE 10
VELOCITY PROFILES

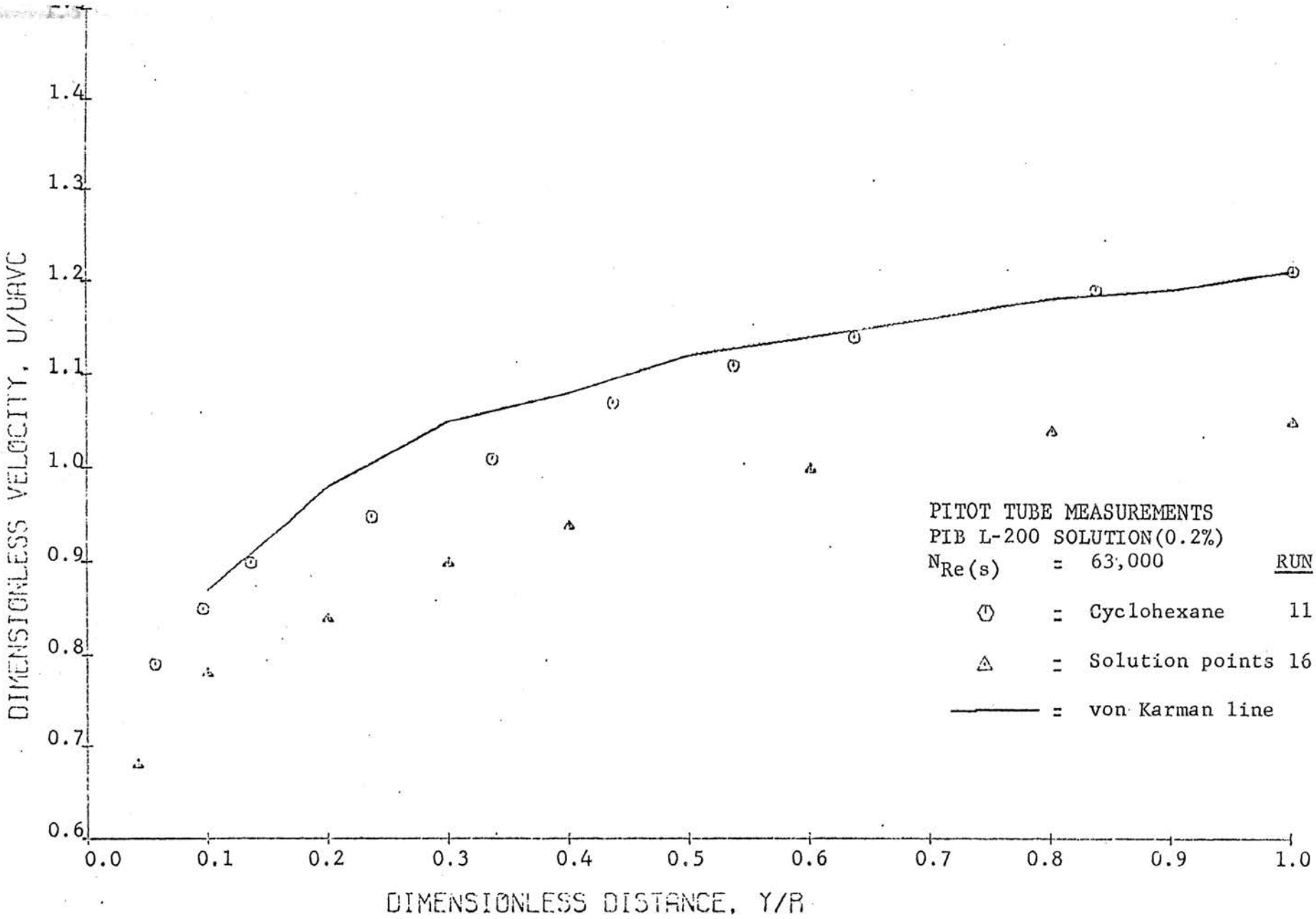

FIGURE 11
VELOCITY PROFILES

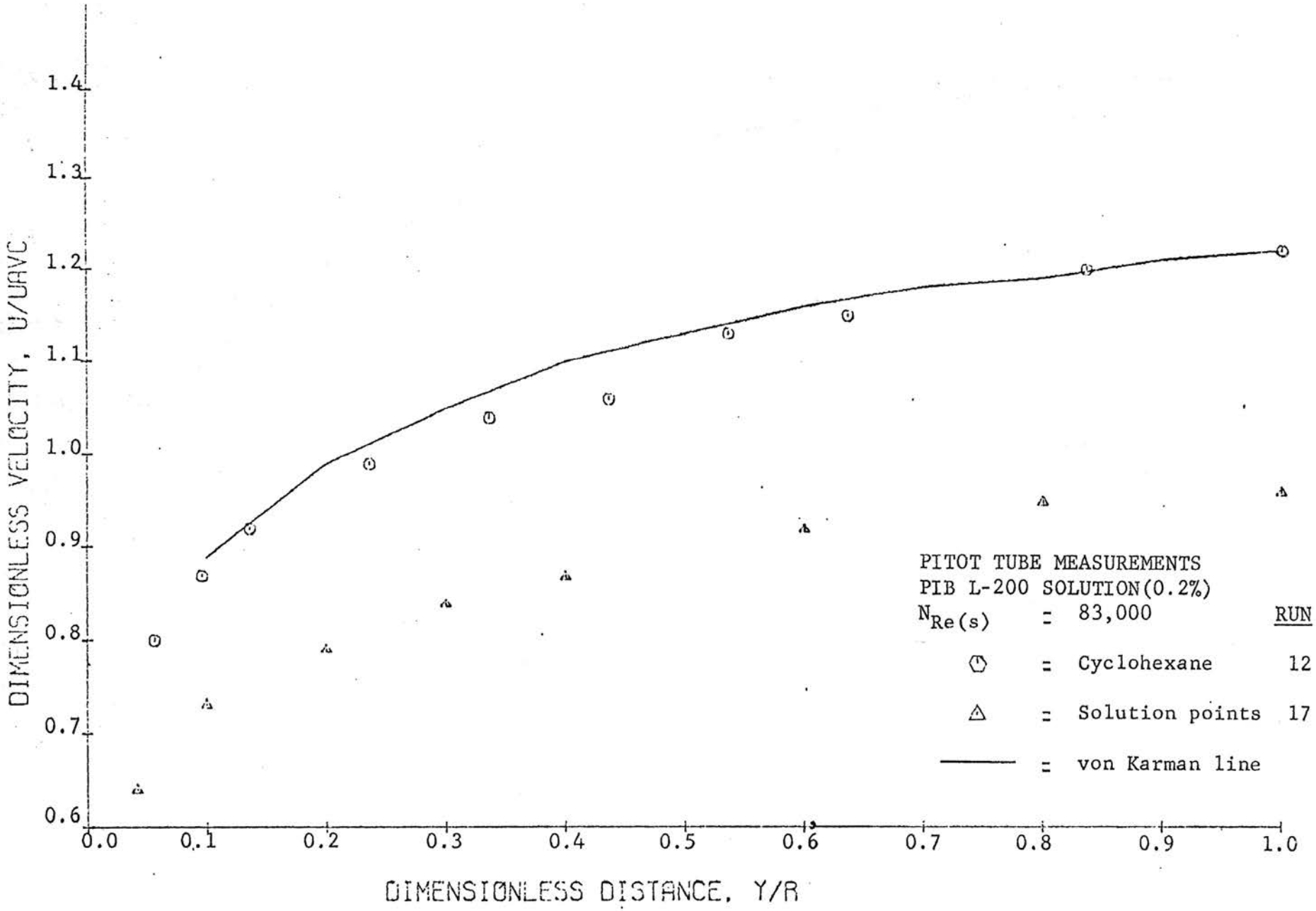

FIGURE 12
VELOCITY PROFILES

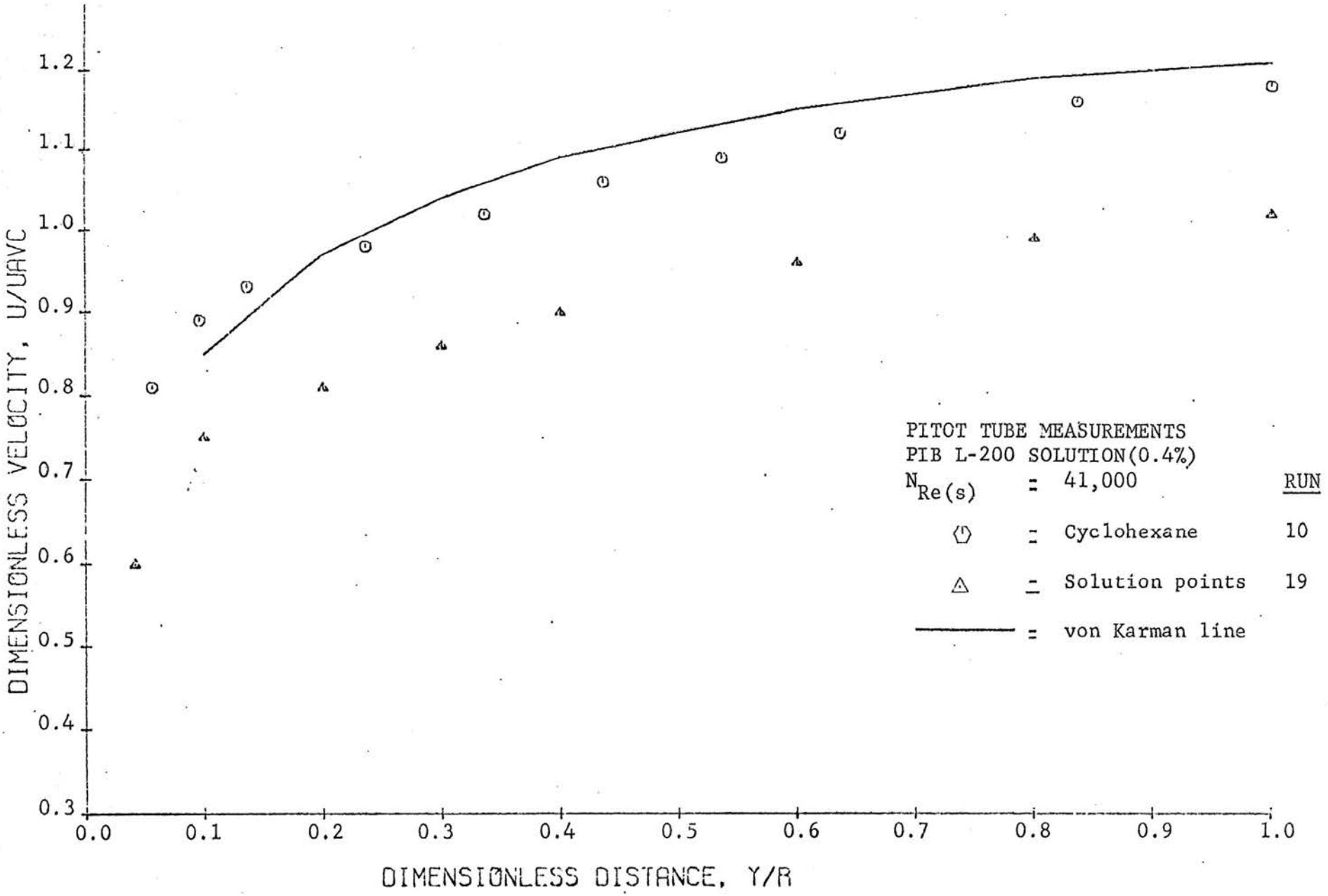

FIGURE 13
VELOCITY PROFILES

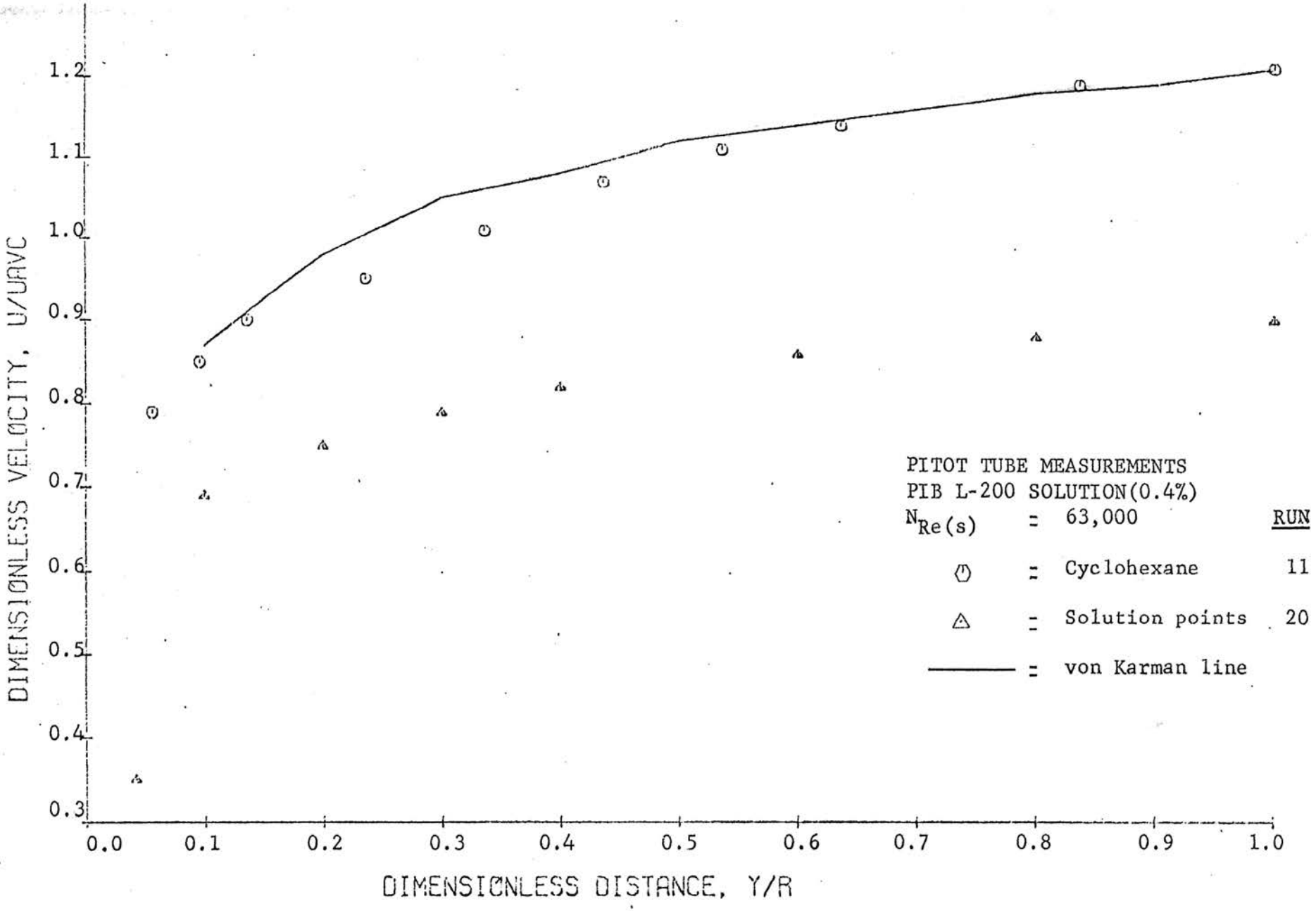

FIGURE 14
VELOCITY PROFILES

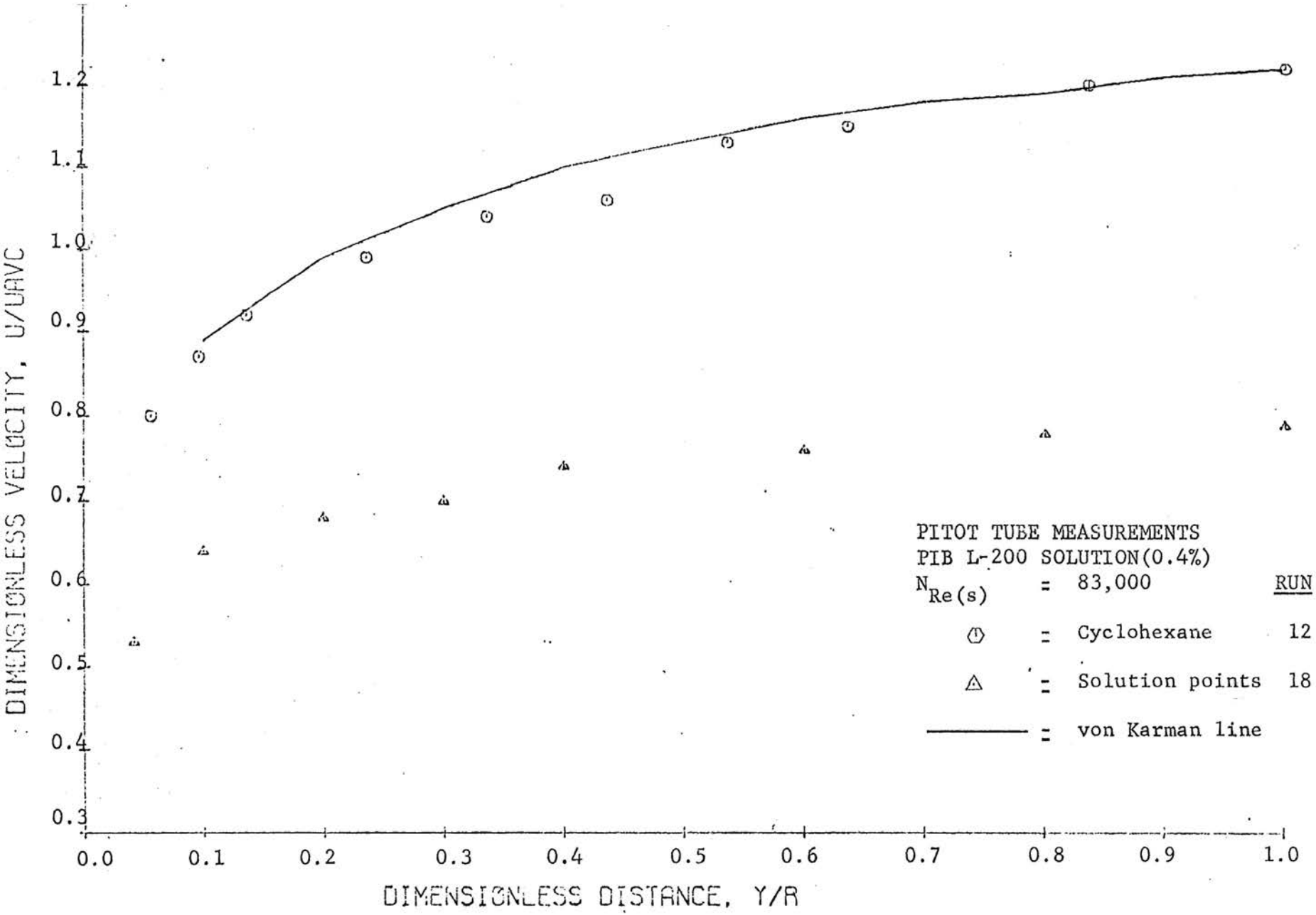

FIGURE 15
VELOCITY PROFILES

TABLE I

FLOW RATE DISCREPANCIES IN VELOCITY PROFILES

Explanation of the symbols used in this table is as follows:

SYMBOL	EXPLANATION
RUN	Run number.
$N_{Re(s)}$	Solvent Reynolds number.
SOLUTE: 2	Solute: Al-Dioleate.
SOLUTE: 1	Solute: PIB L-200.
SOLUTE: 0	Pure Solvent.
SOLVENT: A	Solvent: Toluene.
SOLVENT: B	Cyclohexane.
CONC.	Concentration.
D.R.	Drag Ratio.
SENSOR: X	Pitot tube.
SENSOR: Y	Hot-film anemometer.
UAVC	Average bulk velocity obtained from calibration.
UAVI	Average bulk velocity obtained from integration of the velocity profile.
DEVIATION (%)	Deviation of the average bulk velocity obtained by integration of the velocity profile from the average bulk velocity by weighing (calibration).

TABLE I

FLOW RATE DISCREPANCIES IN VELOCITY PROFILES

RUN	$N_{Re(s)}$	SOLUTE	SOLVENT	CONC.	D.R.	SENSOR	UAVC	UAVI	DEVIATION(%)
1	58000	0	A	0.0	1.000	X	4.91	5.11	3.9
2	104000	0	A	0.0	1.000	X	8.78	8.89	1.2
3	149000	0	A	0.0	1.000	X	12.47	12.72	1.9
4	191000	0	A	0.0	1.000	X	16.14	16.47	2.0
5	221000	0	A	0.0	1.000	X	18.64	18.89	1.3
6	104000	1	A	1.0	0.715	X	8.81	7.82	-11.2
7	148000	1	A	1.0	0.568	X	12.79	11.35	-11.3
8	185000	1	A	1.0	0.539	X	15.64	14.24	-8.9
9	224000	1	A	1.0	0.506	X	18.93	17.38	-8.2
10	41000	0	B	0.0	1.000	X	6.02	5.98	-0.6
11	63000	0	B	0.0	1.000	X	9.35	9.26	-1.0
12	83000	0	B	0.0	1.000	X	12.34	12.43	0.8
13	103000	0	B	0.0	1.000	X	15.30	15.66	2.3
14	123000	0	B	0.0	1.000	X	18.34	18.75	2.2

TABLE I

FLOW RATE DISCREPANCIES IN VELOCITY PROFILES

RUN	$N_{Re(s)}$	SOLUTE	SOLVENT	CONC.	D.R.	SENSOR	UAVC	UAVI	DEVIATION(%)
15	41000	2	B	0.2	0.943	X	6.02	5.42	-10.0
16	63000	2	B	0.2	0.760	X	9.04	7.67	-15.1
17	83000	2	B	0.2	0.725	X	12.33	9.72	-21.1
18	83000	2	B	0.4	0.757	X	12.31	8.21	-33.3
19	41000	2	B	0.4	0.942	X	6.01	4.86	-19.1
20	63000	2	B	0.4	0.760	X	9.02	6.46	-28.4
21	104000	1	A	1.0	0.695	Y	8.82	8.67	-1.7
22	151000	1	A	1.0	0.578	Y	12.50	12.64	1.1
23	41000	0	B	0.0	1.000	Y	6.01	5.90	-1.9
24	61000	0	B	0.0	1.000	Y	9.05	8.84	-2.4
25	83000	0	B	0.0	1.000	Y	12.34	12.01	-2.7
26	41000	2	B	0.2	0.943	Y	6.01	5.86	-2.6
27	61000	2	B	0.2	0.760	Y	9.02	8.78	-2.1
28	83000	2	B	0.2	0.725	Y	12.41	12.22	-1.5

TABLE I

FLOW RATE DISCREPANCIES IN VELOCITY PROFILES

RUN	$N_{Re(s)}$	SOLUTE	SOLVENT	CONC.	D.R.	SENSOR	UAVC	UAVI	DEVIATION(%)
29	41000	2	B	0.4	0.942	Y	6.01	5.83	-3.1
30	61000	2	B	0.4	0.760	Y	9.03	8.91	-1.3
31	83000	2	B	0.4	0.759	Y	12.31	12.56	2.1

AVERAGE ABSOLUTE DEVIATION ON NON-DRAG REDUCING FLUIDS(*) =24.2/13= 1.9

AVERAGE ABSOLUTE DEVIATION ON DRAG REDUCING FLUIDS (HOT-FILM SENSOR) =15.5/8= 2.0

(*) PITOT TUBE AND HOT FILM ANEMOMETER MEASUREMENTS

and for the 1.0 per cent aluminium dioleate solution at different flow rates in a one-inch tube. In each figure, the measured flow rates for the solvent and for the solution are about the same. The measured velocity profiles for the solvent are in good agreement with the von Karman reference lines for the same Reynolds number.

Solution profiles are almost parallel to the solvent profiles, even in regions close to the wall where steeper velocity gradients are present compared with those near the tube axis. However, the local velocities obtained for the solution are always lower than those for the solvent, and the integrated velocity profiles yield lower values in the solution than in the solvent. Good agreements between integrated profiles and measured flow rates were obtained for the solvent (Table I). The average deviation was about 1.4 per cent.

At the four Reynolds numbers studied the solution exhibited drag reduction with drag ratios between 0.715 and 0.506. The low values of the solution velocity profiles are the result of the presence of normal stress differences in the viscoelastic drag reducing solution (1). The elastic contribution, as discussed before, decreases the observed differential pressure reading since its sign is negative. Also, the elastic contribution varies with radius differently with different flow rates.

No correction was applied in the calculation of local velocities from the Pitot tube data for soap solutions, and as described in the experimental procedure only one Pitot tube size

was used. The apparent lack of correlation of the flow rate discrepancies reported in Table I could be explained by the notion of an "optimum" Pitot tube size for drag reducing fluids as advanced by Virk (47). Virk's results seemed to indicate that the flow rate discrepancy was reduced at lower flow rates and with larger Pitot tubes. His results are based on center-line velocity comparisons, however, which might be invalid for the polymer solutions if their profiles were steeper as are some in this investigation. It does not appear that enough data are available to support explanation of the behavior of the flow rate discrepancies.

CYCLOHEXANE - POLYISOBUTYLENE L-200 SYSTEM

Velocity profiles in the PIB L-200 in cyclohexane solutions were measured at two concentration levels, 0.2 and 0.4 per cent, in Runs 15 through 20 shown in Figures 10 through 15.

For this system the shapes of the velocity profiles for the solutions show slightly blunter profiles than do the solvent. The solution profiles are much lower than normal. The difference in shapes is almost negligible at the lowest solvent Reynolds number of 41,000 and increases slightly with increasing flow rate. Even blunter solution profiles can be observed in the more concentrated solution (Figures 13-15). From $y/R = 0.05$ to 0.10 the solution velocity gradient is greater than for the solvent. This effect could be caused by measurement error introduced by the negative contribution of the first normal stress difference, whose value is greater near the wall.

In the 0.2 per cent solution the drag ratio decreases with increasing flow rate, ranging between values of 0.923 and 0.725. Values of (u/UAVGC) also have the same trend and the lack of correlation with flow rate observed in the aluminium dioleate solution is not noticeable. The "optimum" flow rate for the particular Pitot tube size used was probably not approached in these solutions.

The 0.4 per cent solution showed the same Pitot tube effects as the 0.2 percent solution, although these effects were more pronounced. The drag ratio values were about the same for the two solutions at each flow rate level. Because of its greater viscoelasticity, flow rate discrepancies were greater in the more concentrated solution. It is important to point out that these concentrated solutions exhibited non-Newtonian characteristics (35).

The critical or optimum drag reducing concentration at which the drag ratio for the PIB-cyclohexane system is minimum at constant flow rate (in the range studied here), seems to be located between 0.2 and 0.4 per cent PIB L-200. As a result, the addition of polymer to the 0.2 per cent solution to produce a 0.4 per cent solution did not affect the pressure drop at the same flow rate, although effects such as blunter profiles and greater flow rate discrepancies, representing elastic effects, were noticeable in the 0.4 per cent solution. This is a result of the increase in viscosity which limited the drag reduction as discussed by Hershey (15), Rodriguez (35), Patterson

(28), Patterson and Zakin (29), and Rodriguez, Zakin, and Patterson (36).

OVER-ALL PICTURE OF THE PITOT TUBE VELOCITY PROFILE MEASUREMENTS

Local velocities of two viscoelastic drag reducing systems, a soap and a polymer solution, were measured in the turbulent flow region in pipe flow. The shape of the velocity profiles of the solutions and the solvents were only slightly different even for the case of the more non-Newtonian 0.4 per cent PIB L-200 in cyclohexane solution, the major effect being low measured velocities entirely across each profile.

For the Pitot tube velocity profile measurements in the soap solution, a lack of correlation of flow rate discrepancy with flow rate, and hence with drag ratio, indicated that the "optimum" Pitot tube size of Virk (47) might have some validity. The absense of this effect for the PIB-cyclohexane solutions indicated that size effects may be different for each system. Much more investigation will be required to clarify this point.

These observations confirm the inadequacy of Pitot tubes for velocity profile measurements in viscoelastic drag reducing solutions and also point to size effects in the use of Pitot tub sensors as indicators of normal stress differences in laminar flow as suggested by Savins (40). Theoretically, if local velocities for laminar flow of viscoelastic fluids were known,

one could compare these values with Pitot tube measurements, and the difference obtained at the same radial position for a given flow rate would give a quantitative indication of the normal stress contribution. But if Pitot tube size has an effect on the Pitot tube output, values of the normal stresses obtained as described before would be a function of the Pitot tube size.

The drag ratio decreases with flow rate for the soap and polymer systems. It was noticed that lower drag ratios were obtained in the soap system even though less bluntness was observed in the profiles as well as less pronounced flow rate discrepancies. Thus, no simple relation is apparent to describe the behavior of the soap and the polymer solutions; probably because the mechanism governing drag reduction in the polymer system is different from the soap system. It is important to point out that turbulence intensities in these two systems measured by Rodriguez (37) at similar flow rates are also different.

HOT-FILM ANEMOMETER VELOCITY PROFILES

Exploratory measurements of velocity profiles in viscoelastic drag reducing fluids with a hot-film anemometer were made. The same two systems, at the same flow rate levels studied with the Pitot tube, were used. Runs 21 through 31* and figures 16 through 23 represent these profiles. Each figure

*Appendix III

contains the von Karman reference velocity profile line at the solvent Reynolds number, the solution hot-film anemometer velocity profile, and the solvent velocity profile.

TOLUENE-ALUMINIUM DIOLEATE SYSTEM

Figures 16 and 17 represent the profiles for the 1.0 per cent aluminium dioleate in toluene solution in which solvent velocities were measured with the Pitot tube sensor and the solution velocities with the hot-film sensor. Because of the non-Newtonianism of the solution, knowledge of the variation of the viscosity with flow rate was necessary in order to establish a suitable correlation of center velocities with hot-film anemometer voltages. The apparent wall viscosity was used to calculate the Reynolds number to obtain approximate values of $(u/UAVGC)_c$. The flow curve for the flow rate range studied was obtained from measurements made by Radin (32).

The following procedure was used to determine approximate values of viscosity at the desired flow rate:

a) The wall shear stress was calculated from pressure drop measurements.

b) The wall shear stress was divided by the corresponding wall shear rate (from the viscometer flow curve) to obtain the apparent wall viscosity.

The second step to obtain the calibration curve was the choice of an appropriate equation relating center tube velocities with flow rate. This equation was obtained from Nikuradse

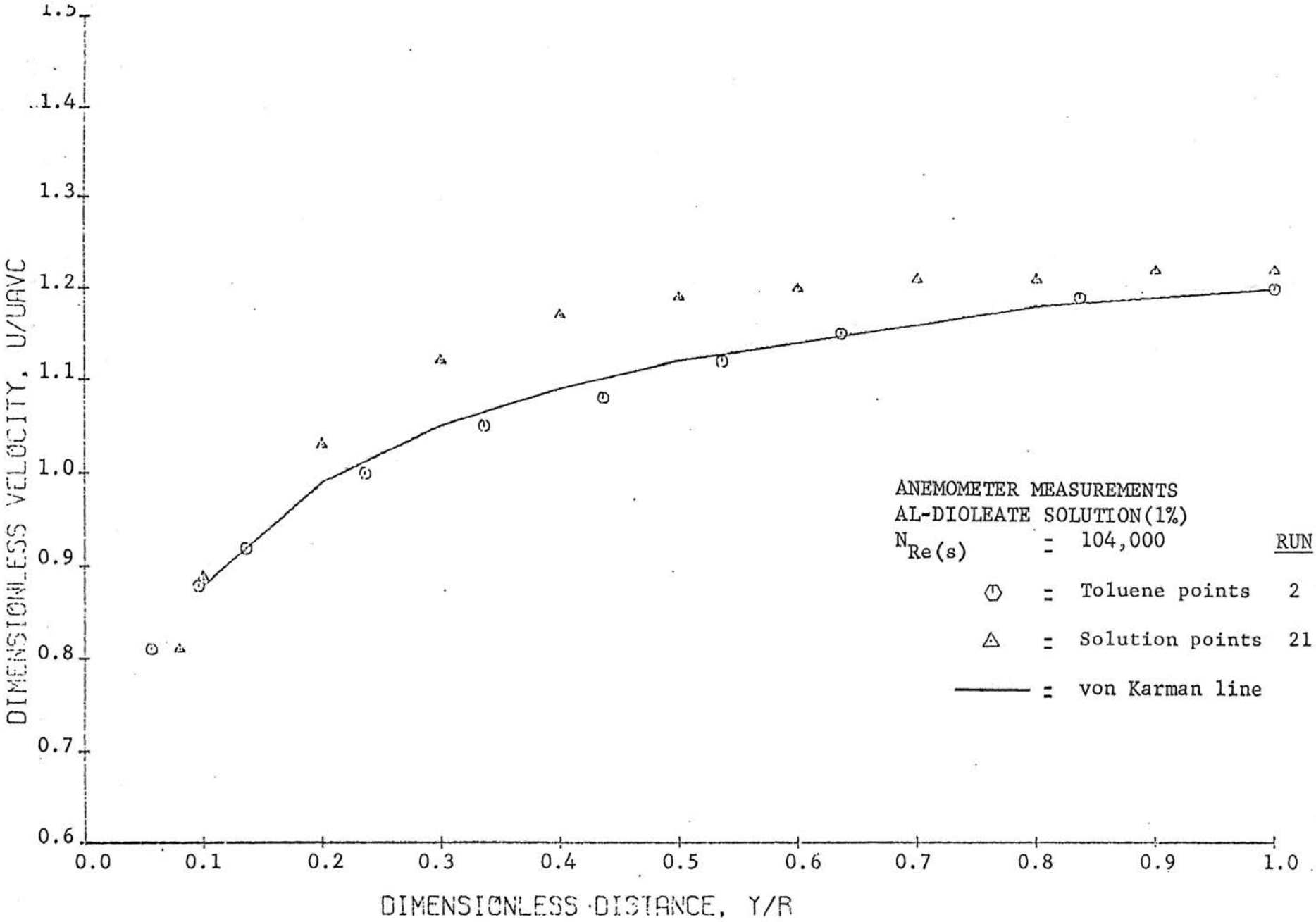

FIGURE 16
VELOCITY PROFILES

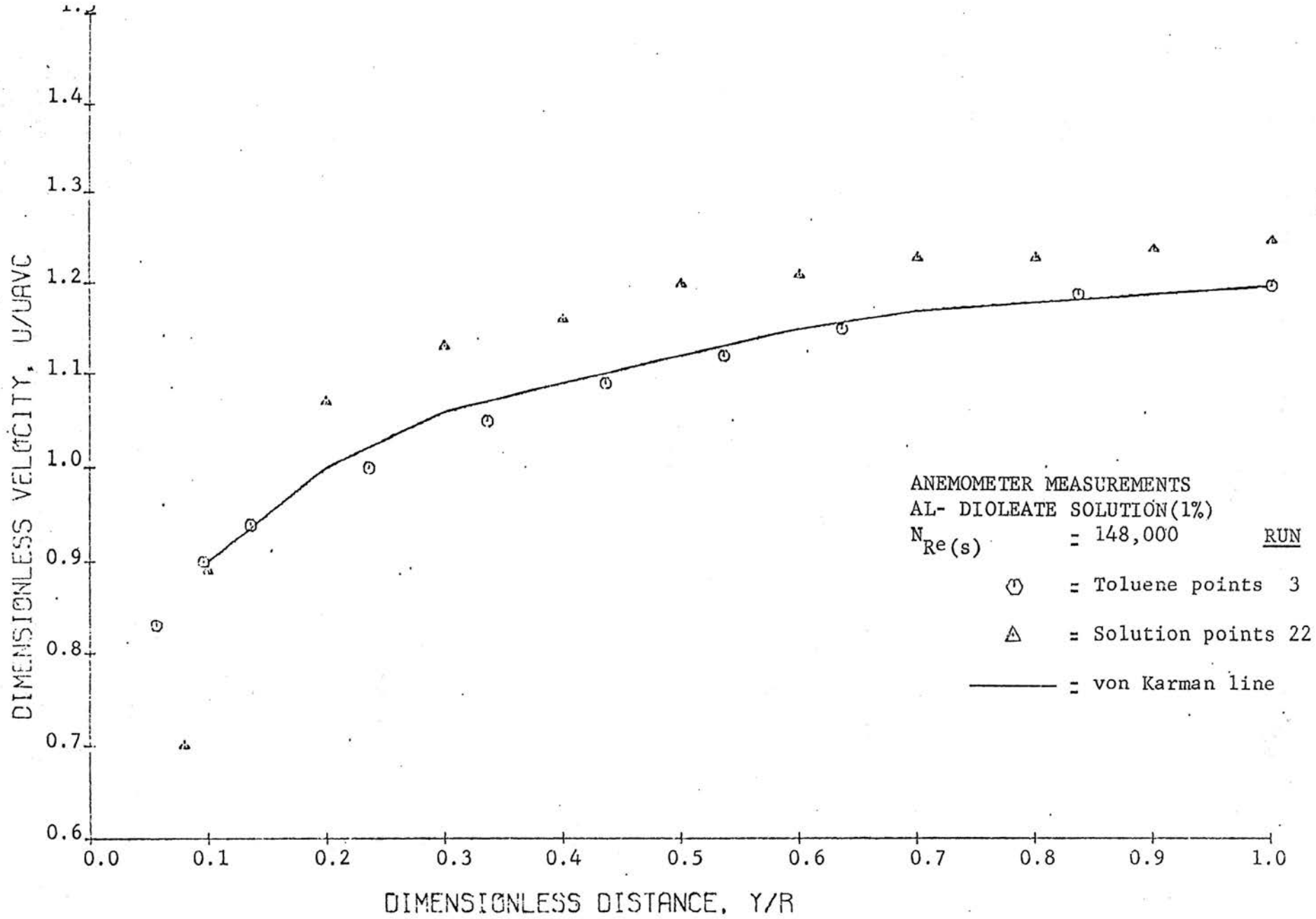

FIGURE 17
VELOCITY PROFILES

data presented in a plot of (u_c/U) versus N_{Re} in Reference (18). These data have a linear form in the Reynolds number range used, so a straight line fit was obtained:

$$u_c = \frac{FR}{\rho(14.81 + 0.92 \log(FR/\mu))} \qquad (22)$$

where FR is flow rate in pounds per minute, ρ is density in g/cc, and μ is the viscosity in centipoises. As seen from the equation, which is only valid for one inch diameter tubes, there is a weak dependence of center velocity on viscosity.

Using this relation with anemometer voltages measured at the tube axis for various flow rates, a least square-best-fit-equation for u versus E was determined (see Appendix I). The equation used was a function of the specific fluid and was different for each profile.

There was no sharp difference as seen in Figures 16 and 17, between the velocity profile shapes for the solution and for the solvent. Local velocities were greater in the solution, with the exception of the closest points to the wall. Since this type of sensor responds only to velocity effects on heat transfer (which have been directly calibrated), normal stress differences should not influence the measurement.

Table I shows the comparison of the average velocities from the anemometer measurements and flow rate measurements obtained by weighing. Fairly good agreements were obtained.

In this system, a small but consistent drift in the calibration curve was observed by comparing the center line anemometer voltages before and after the profile. For this reason correctio

factors for local voltages were applied before calculating local velocities. The drag ratio levels were about the same as in the corresponding Pitot tube measurements, and no appreciable degradation of the solution was noticed.

CYCLOHEXANE-POLYISOBUTYLENE L-200 SYSTEM

The same two concentrations of PIB L-200 in cyclohexane as in the Pitot tube measurements (0.2 and 0.4 per cent) were used for hot-film anemometer velocity profile measurements. Figures 18 through 23 show these profiles.

The local velocities measured with the hot-film anemometer in the solvent are about the same and depict similar profiles if compared with Pitot tube profiles. Also, von Karman reference lines agree fairly well with the experimental velocity values, and average velocity checks for these velocity profiles are within experimental error .

The calculation of center velocities for calibration curves followed the same method outlined for the soap solution with the exception that flow curves for the solutions were not available, so approximate viscosities were used (see Appendix III, Table IV). The checks of center voltages for calibration curves were also made for this system, and if some drift was noticed appropriate corrections were made.

The 0.2 per cent solution measurements with the hot-film were made before the Pitot tube measurements. Great difficulty was experienced in obtaining reliable values when the solution

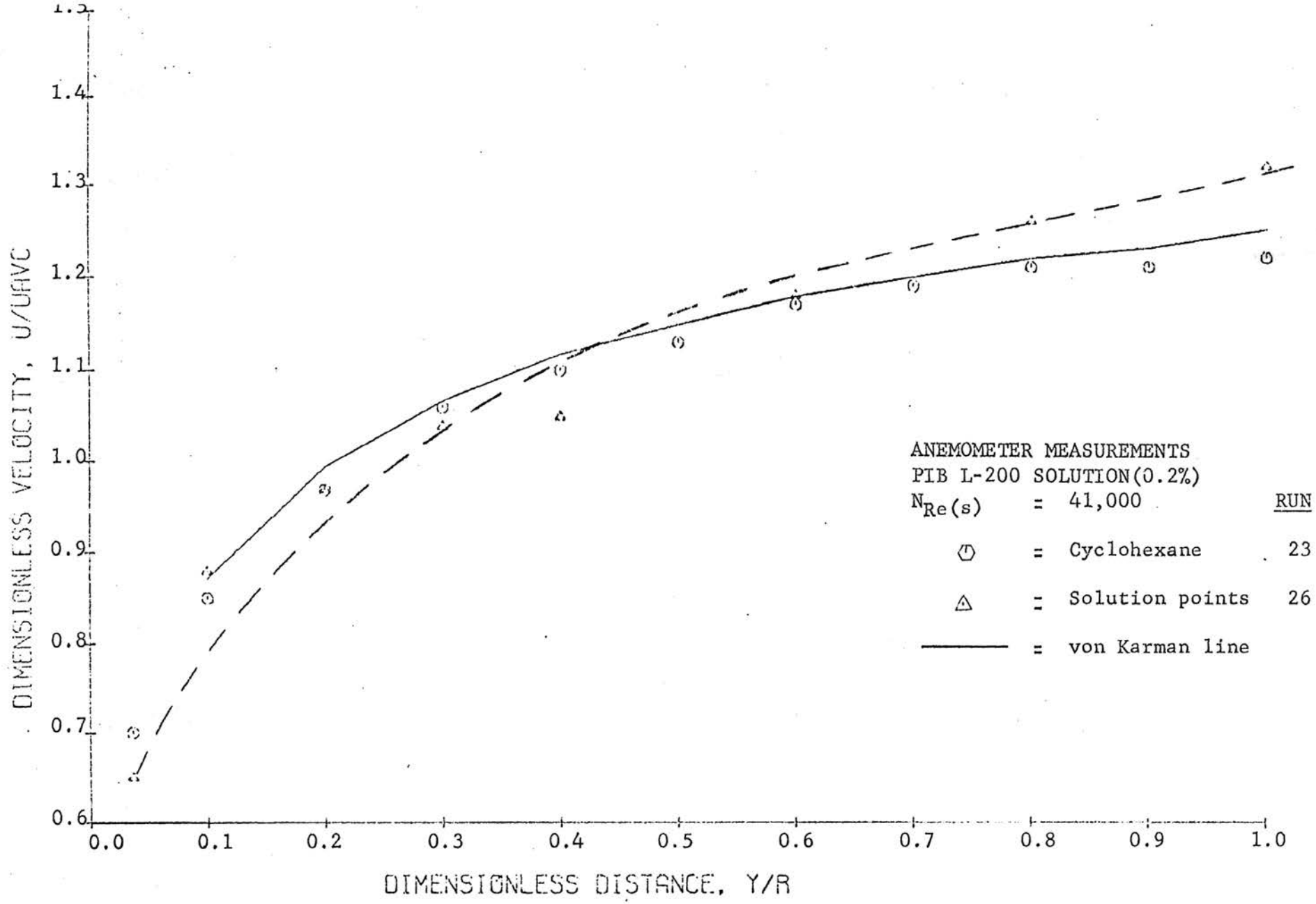

FIGURE 18
VELOCITY PROFILES

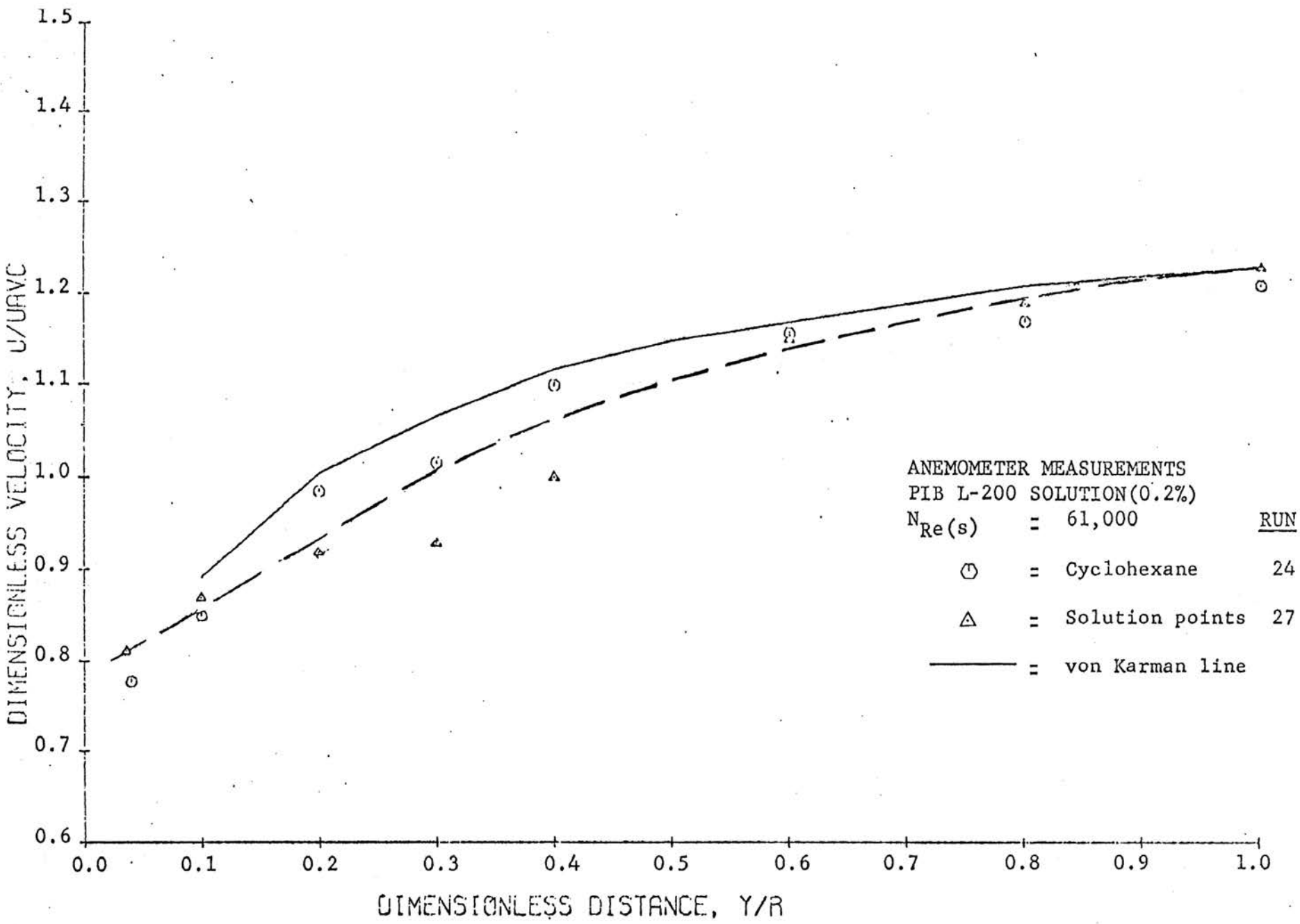

FIGURE 19
VELOCITY PROFILES

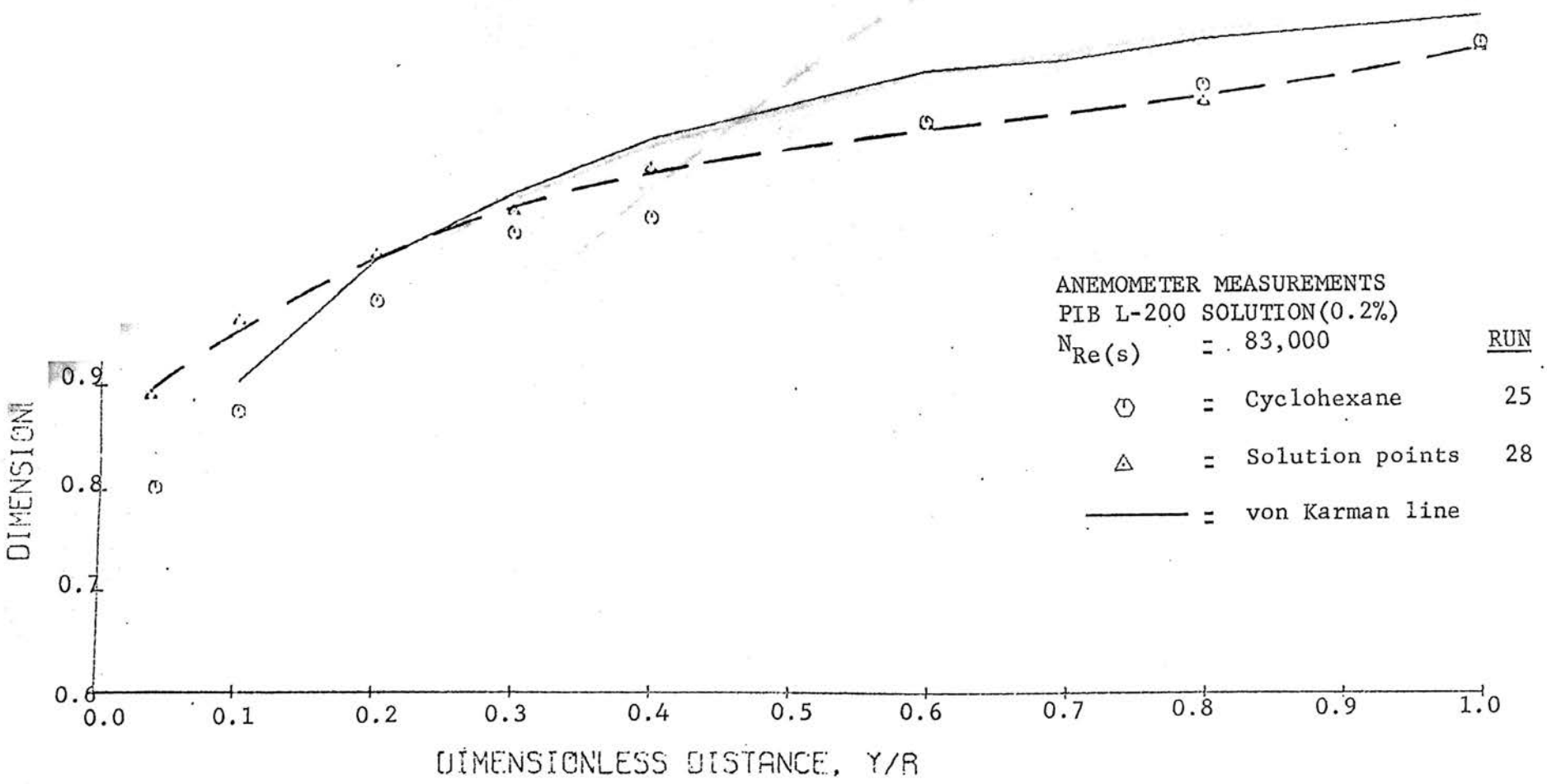

FIGURE 20
VELOCITY PROFILES

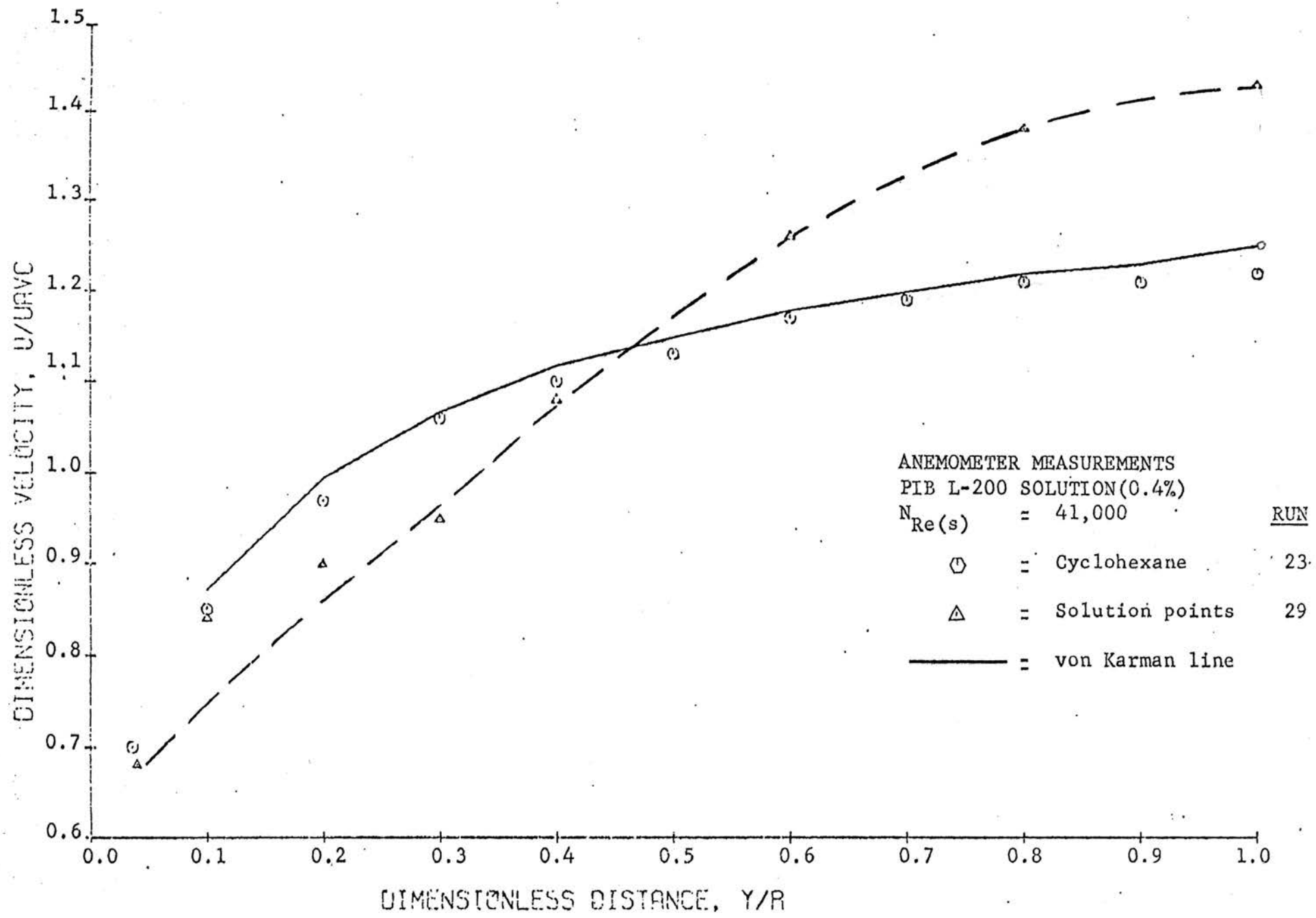

FIGURE 21
VELOCITY PROFILES

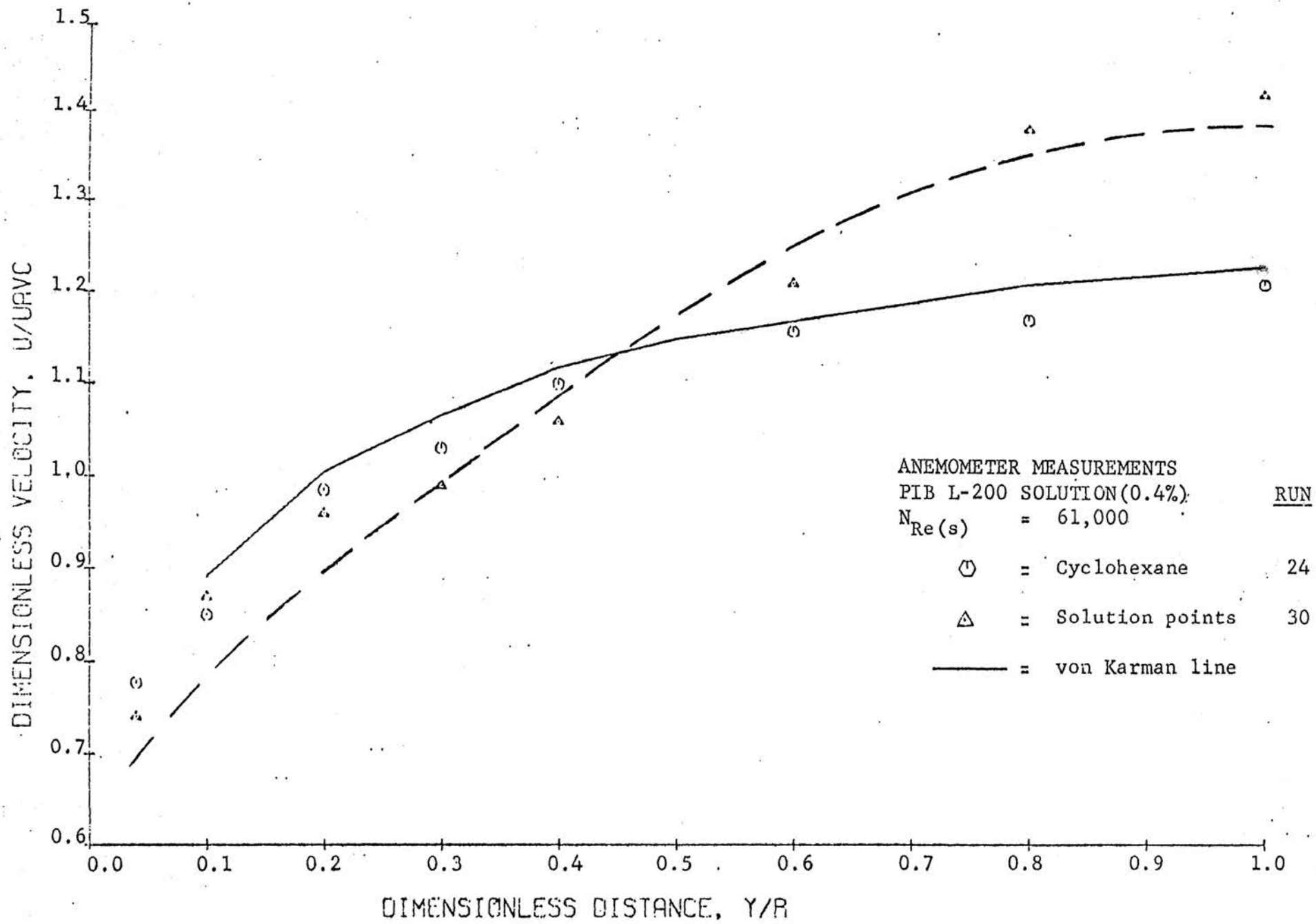

FIGURE 22
VELOCITY PROFILES

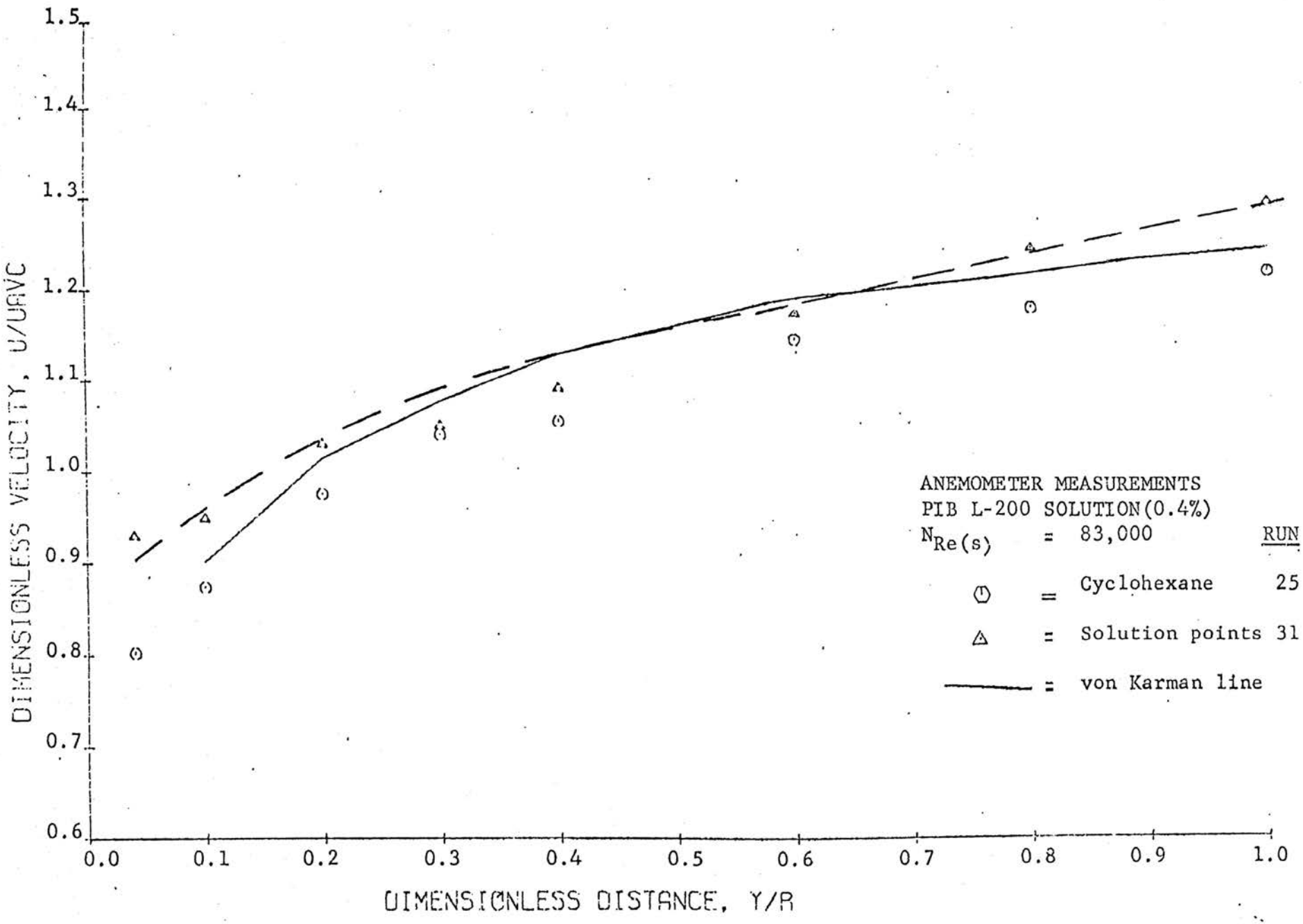

FIGURE 23
VELOCITY PROFILES

was fresh. At that time, the voltage dependence on velocity was confounded by anomalous voltage changes. Only after a considerable pumping time, did voltages remain reasonably stable and were average velocity checks obtained.

At the lowest flow rate used for the 0.2 per cent solution, there was a marked change in slope of the velocity profile, as observed in Figure 18, and steeper velocity gradients near the center region are present if compared with solvent velocity gradients. At the intermediate and high flow rates the behavior of the profiles close to the center region is similar to the solvent profiles. Also, lower local velocities are present close to the wall, and their value decreases as flow rate increases; which is equivalent to an increase of the viscous boundary layer thickness with increasing flow rate (see Figure 24). In general, at the flow rates used, local velocities in the solution are higher than solvent velocities in regions close to the wall ($y/R \leq 0.1$), as well as in regions close to the center ($y/R \geq 0.6$), with lower intermediate values.

A graphical procedure for determination of the local velocities on the basis of local voltage measurements was devised for the 0.4 per cent solution, since the least square best-fit-equations from calibration curves gave erroneous values for center velocities. A plot of center voltages and center velocities was drawn on a large scale graph. From this calibration curve, values of local velocities were obtained from local voltage measurements.

The behavior of the velocity profiles in this solution was quite different from the 0.2 per cent solution. Steeper profiles were present giving high tube center velocities for a given bulk mean velocity. Because of this effect the (u_c/U) correlation used previously for calibration of the anemometer was no longer valid. Its use, however, to calculate the velocity profiles showed that they were about 12 per cent low at all three velocities, so appropriate corrections in (u_c/U) values were made in the final calculations.

The high center tube velocities could be caused to a small extent by a Reynolds number effect, since the solution Reynolds numbers were lower than for the solvent. The main explanation for the high center velocities and high velocity gradients in the drag reducing PIB L-200 solutions, however, must be the viscoelastic effects of the solute (not to be confused with the apparent effects on velocity profile caused by normal stresses when Pitot tubes are used for measurement).

Velocity profile measurements in viscoelastic polymer solutions with the cylindrical hot-film anemometer were made somewhat difficult by the great decrease in heat transfer rate from the hot-film in the solutions as compared to the solvents. This caused voltage variations with velocity to be much smaller than desirable. The same effect was discussed by Marrucci and Astarita (20), and Lindgren and Chao (19). Heat transfer rate reduction is greater than drag reduction at the same flow rate for viscoelastic fluids.

OVER-ALL PICTURE OF THE HOT-FILM ANEMOMETER MEASUREMENTS

A clear difference in the velocity profile shapes for the soap and polymer systems is present. The soap profiles have shapes similar to solvent profiles and at the two flow rates used, solution profiles in this system are slightly blunter. On the contrary for the polymer system the profiles are in general steeper than solvent profiles. There is no clear relation between the shapes of the profiles for the non-polymer and polymer systems.

Good average velocity checks were obtained in all the measurements with the hot-film sensor, which indicates that velocity measurements by this technique are reliable.

Figure 24 shows a law of the wall plot (u^+ versus log y^+) obtained from hot-film anemometer measurements. The viscosity at the wall was evaluated using shear stress-shear rate data from capillary viscometer measurements made by Radin (32) for the aluminium dioleate solution, and made by Rodriguez (35) for the cyclohexane-PIB L-200 solutions. Even though the solutions used by Rodriguez were made-up at different times from those used in this investigation, his data was used to draw the flow curve in order to obtain an approximate value of the wall viscosity of the solution. The function plotted was a logarithmic function and small changes in the value of the viscosity at wall conditions affected the value of log y^+ very little, so a good approximate comparison of the data was obtained in this kind of plot.

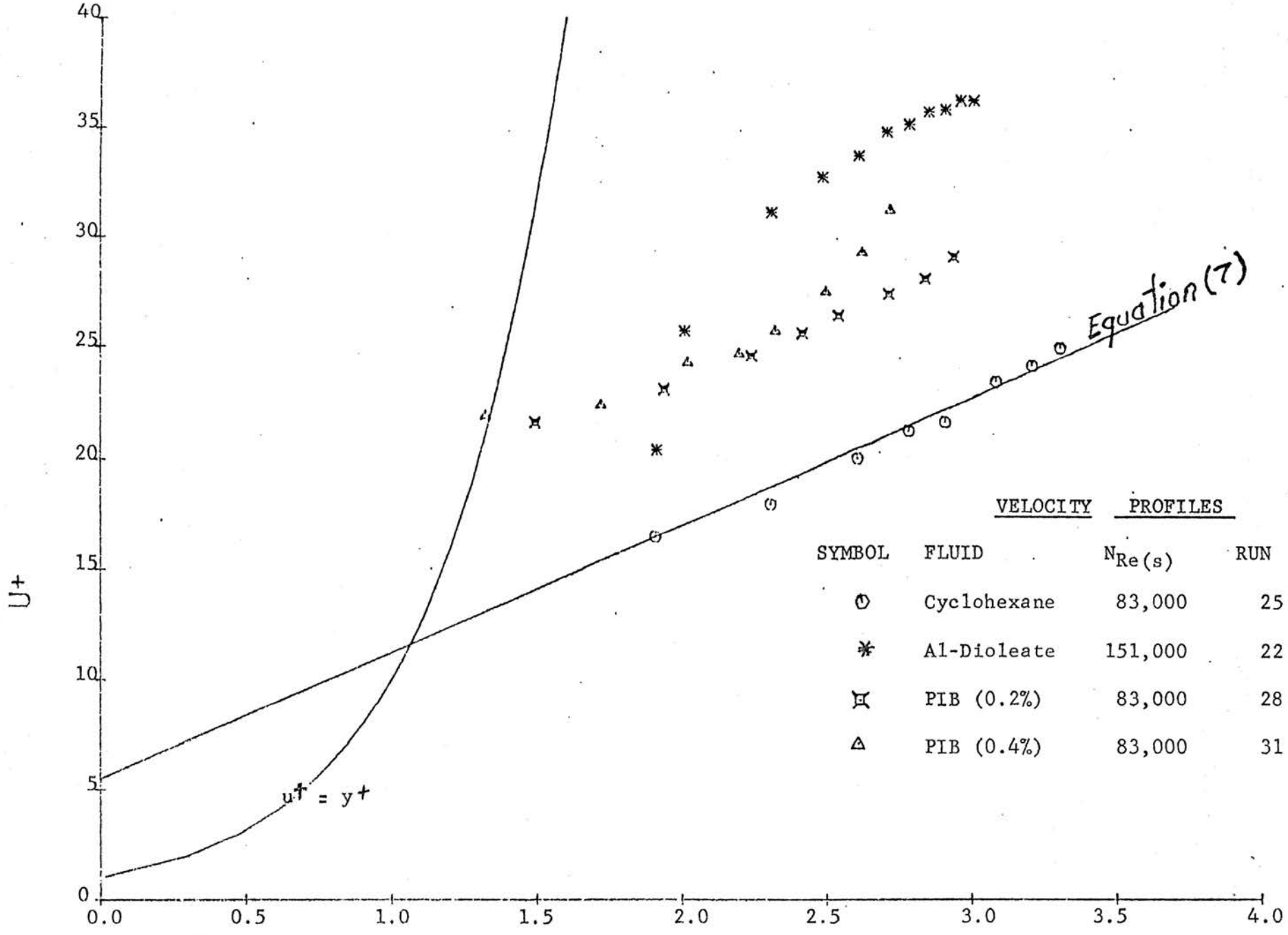
40
35
30
25
20
15
10
5
0
U+
0.0
0.5
1.0
1.5
2.0
2.5
3.0
3.5
4.0
LOG Y+
u+ = y+
Equation (7)
VELOCITY PROFILES
SYMBOL FLUID $N_{Re(s)}$ RUN
Cyclohexane 83,000 25
Al-Dioleate 151,000 22
PIB (0.2%) 83,000 28
PIB (0.4%) 83,000 31

FIGURE 24

The reference line for Newtonian fluids obtained from equation 11 was compared in Figure 24 with the hot-film anemometer velocity profiles of cyclohexane and with the polymer and soap systems at the highest Reynolds numbers. Cyclohexane points fit the reference line fairly well. In the drag reducing polymer solution profiles the thickness of the boundary layer is seen to be greater than for Newtonian fluids, and the profile points are located well above the Newtonian reference line. Wells (49) observed the same behavior for his viscoelastic solution profiles of J-2P and CMC-70 in water, even though his profiles were an average of 6 per cent low. Since his measurements were obtained by impact tube techniques which were affected by normal stress differences, the true u^+ values for his solutions must be even higher at the same flow rate. Ernst (12) also obtained this result in 0.05 per cent CMC solutions. The u^+ values for the 0.2 per cent PIB L-200 solution and for the Al-dioleate solution were much greater than the Newtonian reference line because the wall shear stresses were much lower than normal, giving low u* values.

Although the flow rates for the velocity profiles of the 0.2 and 0.4 per cent polymer solutions were alike, higher u^+ values for given y^+ values were observed in the 0.4 per cent solution. This effect was primarily a result of the higher viscosity in the 0.4 per cent solution, causing lower values of y^+ at given pipe locations.

The $u^+ - y^+$ behavior of the Al-dioleate solution was not the same as for the polymer solutions. Thicker boundary layers do not seem to be indicated, but the transition from turbulent to viscous regions is different from the transition for solvents and polymer solutions. More data will be necessary to clearly describe the soap solution profiles in the transition region.

VI CONCLUSIONS

a) There are discrepancies between flow rates evaluated from calibration and flow rates evaluated from integration of local velocities measured with the Pitot tube in viscoelastic drag reducing fluids. These discrepancies are caused by normal stress differences and are a function of the following factors:

1) drag reducing level
2) concentration of the additive in the viscoelastic solution
3) Pitot tube size
4) Reynolds number

b) Flow rates obtained by integration of hot-film velocity profiles have indicated that correct values of local velocities in viscoelastic drag reducing fluids can be obtained by that method. The measured values were not affected by normal stress differences.
Table II shows discrepancies in flow rates for velocity profile measurements in this study compared with those of other investigators.

c) Hot-film anemometer velocity measurements indicate that an increase of the boundary layer thickness is present in the turbulent flow of drag reducing polymer solutions, but the soap solutions showed a different type of transition region which was difficult to interpret.

TABLE II

COMPARISON OF DISCREPANCIES IN FLOW RATES FOR VELOCITY PROFILE MEASUREMENTS

INVESTIGATOR	NUMBER OF PROFILES	AVERAGE ABSOLUTE DEVIATION (%)	ALGEBRAICALLY SUMMED DEVIATIONS (%)*
Shaver (43)	8	6.1	-6.0
Bogue (3)	27	1.5	
Eissenberg (10)	4	2.7	
Wells (49)	10	4.6	-2.8
Hershey (15)	25	1.5	
Florez	13**	1.9	0.6
Florez	8***	2.0	-1.2
Florez	10****	16.7	-16.7

* Algebraic sums of deviations from measured flow rates divided by number of profiles measured in viscoelastic solutions.

** Measurements with Pitot tube and hot-film anemometer on non-drag reducing fluids.

*** Measurements with hot-film anemometer on viscoelastic drag reducing solutions.

**** Measurements with Pitot tube on viscoelastic drag reducing fluids.

d) The drag reducing soap solution showed only slight flattening of the velocity profiles in the central region of the tube.

e) The drag reducing PIB L-200 solutions showed steeper velocity profiles in the central region of the tube which became steeper both with flow rate and with polymer concentration.

f) The differences in soap solution and polymer solution velocity profile behavior and the differences in turbulence intensity behavior observed by another investigator suggest that different mechanisms, or at least different modes, of drag reduction are occurring.

VII RECOMMENDATIONS

It is recommended that simultaneous measurements of local velocities in drag reducing viscoelastic fluids with Pitot tube and anemometer techniques be obtained in turbulent flow, since drag reduction is a time dependent effect.

It is recommended that other geometric shapes of anemometer sensors (i.e. hot-wires) be tested, in order to determine the effect of size and configuration of these sensors on local velocity measurements.

It is recommended that measurements of velocity profiles in viscoelastic drag reducing solutions in a wide range of Pitot tube sizes be made, in order to analyze the effect of sensor size on errors in velocity measurements.

VIII APPENDICES

APPENDIX I

HOT-FILM ANEMOMETRY

The measurement of the velocity of a fluid by anemometry techniques is based on the variation of the heat transfer rate from a hot surface with fluid velocity. The total heat transfer rate is also a function of the temperature difference between the hot surface and the bulk fluid as well as being dependent on the physical properties of the fluid and the surface (film, wire, or other geometric type).

The hot-film anemometer sensor characteristics are determined by its material, shape and length. Its heat losses, when immersed in a fluid, consist of contributions of radiation, in parallel with natural and forced convection and conduction through the fluid layer close to the hot film surface in series with convective heat transfer.

Several equations are found in the literature correlating heat transfer variables as a function of fluid velocity (17). Their use is limited by the type of fluid used and Reynolds number range involved.

For experimental use an equation can be written in terms of the variables governing the electric heating and the convection cooling of the sensor as follows:

$$\frac{R}{R_o} I^2 = A + B(u)^n \qquad (1A)$$

where I is the heating current, R is the operating resistance of the sensor, R_o is the resistance of the sensor at fluid temperature A,B and n are constants

This equation may be written also as:

$$E^2 = A' + B' (u)^n \qquad (2A)$$

where E is the voltage impressed on the sensor. When the exponent n in equation (1A) equals 0.5, the expression is called King's law (17).

Expression 2A is a suitable correlation to fit experimental data when velocity profile measurements are to be made, although this expression does not usually fit an entire calibration curve. A least-square-best-fit procedure must be used to obtain the constants A', B' and n.

Basically two modes of operation are used in anemometry--the constant current and the constant temperature modes. Reference 17 discusses the approach to the constant current mode.

The constant temperature mode, used in these experiments, maintains operation at constant sensor resistance. To accomplis this

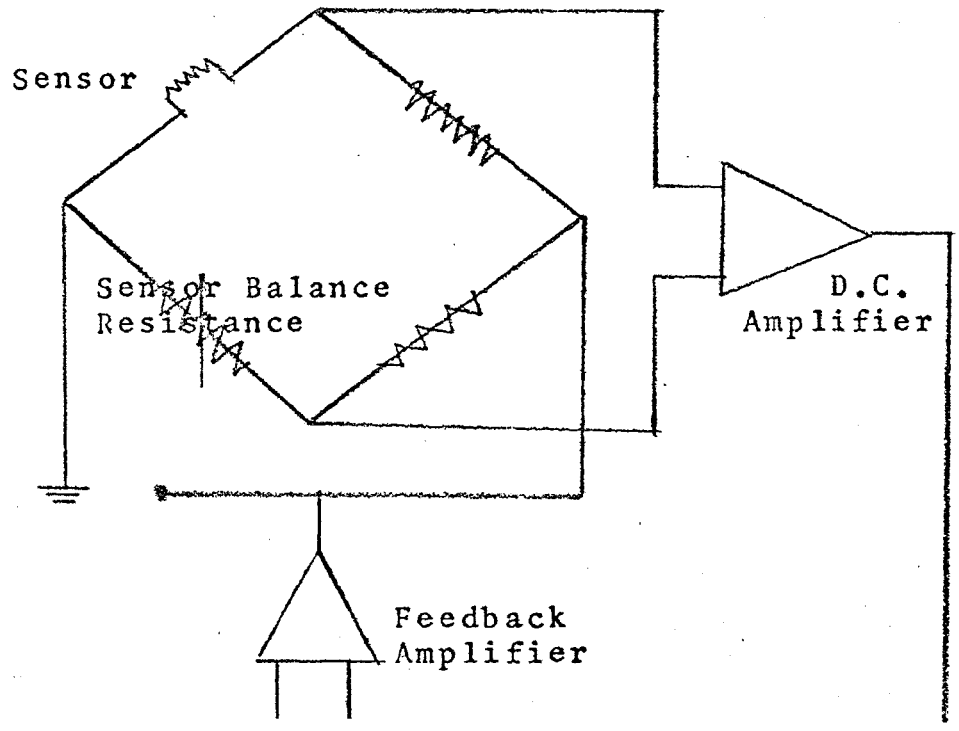

the bridge current is varied with fluid velocity to obtain an adequate heat balance on the sensor. The purpose of the bridge unbalance amplifier, used to control a feedback amplifier which varies the bridge current, is to achieve high frequency response for turbulence measurements.

REASON FOR THE USE OF HOT-FILM ANEMOMETER.

The primary reason for the use of the hot-film anemometer for velocity profile measurements in drag reducing solutions is its insensitivity to normal stress differences. As indicated in the literature review, the use of Pitot tubes will not yield accurate profiles in solutions with high normal stress differences in shear.

Figure 25 shows a typical calibration curve taken in the 0.2% polyisobutylene solution in cyclohexane (Run 28). Table III shows the values of voltage obtained at the tube axis, mass flow rate, and estimated axial velocity. As discussed before center velocities were calculated from equation 22. The best fit from a regression analysis is given for this run by the equation:

$$u = \left(\frac{E^2 - A}{B} \right)^{1/C} \qquad (1B)$$

where A = 155.464

B = 74.320

C = 0.500

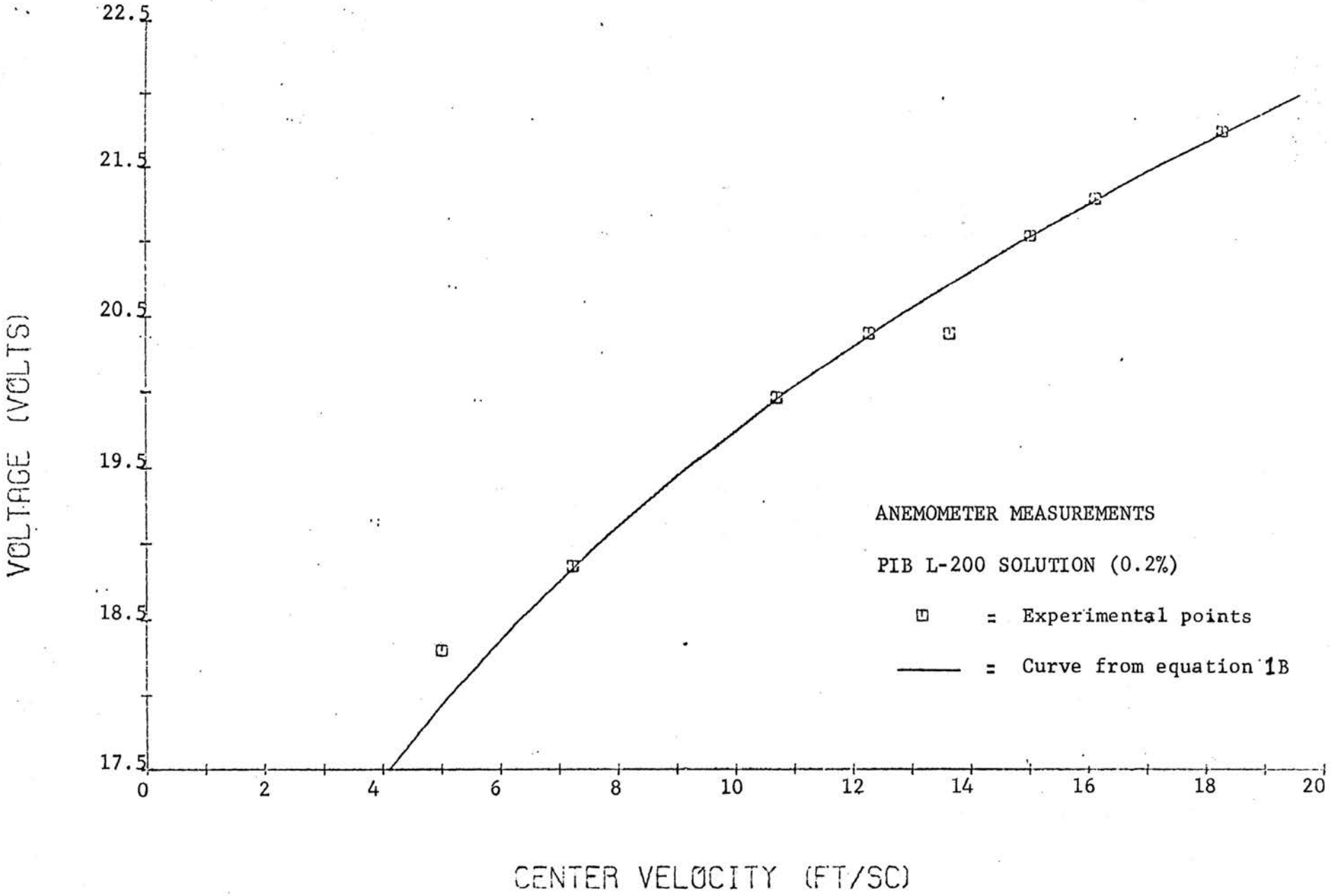

FIGURE 25 CALIBRATION CURVE EXAMPLE

TABLE III

DATA FOR LEAST SQUARE BEST FIT CALIBRATION CURVE

CENTER VOLTAGES (volts)	FLOW RATE (#/min.)	CENTER VELOCITY* (ft /sec)
18.30	73.48	5.77
18.86	95.00	7.42
19.97	136.40	10.57
20.40	156.50	12.09
20.74	175.60	13.52
21.05	196.00	15.01
21.30	215.00	16.48
21.75	232.00	17.79

*Calculated values from equation 22.

APPENDIX II

SAMPLE CALCULATIONS

The majority of the calculations of the present investigation were done on an IBM 360-50 computer. The regression analysis programs used for the calibration curves of the anemometer measurements were written by Dr. H. C. Hershey and Dr. G. K. Patterson. The other programs were written by the author.

An example of the evaluation of the variables studied follows.

For measurements in the one inch tube test section the following experimental values were recorded:

Pitot Tube Measurements

Fluid: Cyclohexane

Run number: 12

Flow rate: 195.4 #/min

Fluid temperature: 25.0°C

Length of the one inch test section: 200.0 inches (between taps)

Fluid density: 0.7749 gr/cc (Appendix III, Table IV)

Fluid viscosity: 0.8892 cp (Appendix III, Table IV)

Total pressure drop: 434.9 lb/ft^2

Impact pressure head at y = 0.5 inches (axis) = 1.178 psi

1) Average Velocity from Flow Rate Measurements

$$U = \frac{Q}{A} = \frac{(\#/min) \times (min/sec) \times (ft^3/lb)}{ft^2} = ft/sec$$

$$= \frac{(195.4)(1/60)(1/0.7749 \times 62.43)}{\frac{\pi}{4} \times \left(\frac{1}{12}\right)^2} = 12.345 \text{ ft/sec}$$

2) Solvent Reynolds Number:

$$N_{Re} = \frac{\rho UD}{\mu} = \frac{(\text{lb-m/ft}^3)(\text{ft/sec})(\text{ft})}{(\text{lb-m/ft} \times \text{sec})} = \text{dimensionless}$$

$$= \frac{(0.7749 \times 62.43)(12.345)(1/12)}{(0.8892 \times 6.72 \times 10^{-4})} = 83000$$

3) Fanning Friction Factor:

$$f = \frac{D\Delta P/4L}{\rho U^2/2} = \frac{(\text{ft})\ \frac{\text{lb}}{\text{ft} \times \text{sec}}\ /(\text{ft})}{(\text{lb/ft}^3)(\text{ft/sec})^2} = \text{dimensionless}$$

$$= \frac{(1/12)(434.9 \times 32.174)/(4 \times 200/12)}{(0.7749 \times 62.43)(12.345)^2/2} = 0.00474$$

4) Fanning Friction Factor from von Karman Equation:

Using equation (14) with n' = 1, and Newton's iteration procedure, the friction factor can be calculated as $f_{vk} = 0.00467$.

5) Local Velocity at axial position:

$$\bar{u} = \frac{2\Delta P g_c}{\rho} = \frac{(\text{lb-m/ft} \times \text{sec}^2)^{1/2}}{(\text{lb-m/ft}^3)^{1/2}} = \text{ft/sec}$$

$$= \frac{2 \times 1.178 \times 144 \times 32.174}{0.7749 \times 62.43} = 15.022 \text{ ft/sec}$$

6) Dimensionless Radius:

$$\frac{y}{R} = \frac{0.5}{0.5} = 1.0$$

7) Dimensionless Velocity (normalized with calibrated average velocity):

$$\frac{u}{U} = \frac{15.022}{12.345} = 1.217$$

8) Dimensionless Velocity (normalized with axial velocity):

$$\frac{u}{u_c} = \frac{15.022}{15.022} = 1.0$$

9) Friction Velocity:

$$u^* = U\sqrt{f/2} = 12.345\sqrt{\frac{0.00474}{2}}$$

$$= 0.60157 \text{ ft/sec}$$

10) UPLUS (dimensionless):

$$u^+ = \frac{u}{u^*} = \frac{15.022}{0.60157} = 24.972$$

11) YPLUS (dimensionless):

$$y^+ = \frac{u^*\rho y}{\mu} = \frac{(\text{ft/sec})x\ \frac{\text{lb}}{\text{ft}^3}\ x(\text{ft})}{(\text{lbxft/sec})} = \text{dimensionless}$$

$$= \frac{(0.60157)(0.7749x62.43)(0.5/12)}{(0.8892x6.72x10^{-4})} = 2029$$

12) Integrated Average Velocity:

For the evaluation of this quantity, from local velocity measurements with Pitot tube, the trapezoidal integration rule was used. The result for this run was:

U = 12.43 ft/sec

Hot-Film Anemometer Measurements

Calibration Curve:

An example of the calibration procedure is given in Appendix I. From that equation, obtained by a regression analysis procedure, voltage and velocity are correlated by the equation:

$$u = \left(\frac{E^2 - 155.464}{74.32}\right)^{1/0.5}$$

Thus, readings of local voltages through different radial positions are applied to this equation to obtain u, i. e. for y = 0.4 and E = 20.93 (Run 28):

$$u = \left(\frac{(20.93)^2 - 155.464}{74.32} \right)^{1/0.5} = 14.46 \text{ ft/sec}$$

The graphical procedure used to determine the correlation between voltage and velocity in runs where regression analysis was not applied is discussed in the analysis of the data section.

APPENDIX III

TABLE IV

PHYSICAL PROPERTIES OF FLUIDS

A. Solvent Densities

Temp.	Solvent	Density	β_0*	β_1*
°C		gr/cc		
25	Cyclohexane	0.7749	0.79707	-0.0008879
30	Toluene	0.8564	0.88412	-0.0009225

*Density = $\beta_0 + \beta_1 T$; T in °C

B. Solvent and Solution Viscosities

Solute	Solvent	Conc.	Viscosity	Temp.
		%	cp	°C
None	Toluene	0	0.551	26.5
Al-disoap	Toluene	1.0	1.456**	26.5
None	Cyclohexane	0	0.889	25.0
PIB L-200	Cyclohexane	0.2	1.350***	27,8
PIB L-200	Cyclohexane	0.4	3.80****	25.0

**Average value in shear rate range of interest (10^4 - 10^5 sec^{-1}) from data of Radin (32)-slightly non-Newtonian.

***Average value in shear rate range of interest--

nearly Newtonian.

****Average value in shear rate range of interest from data of Rodriguez (35)-slightly non-Newtonian.

TABLE V

RAW DATA

The following pages present the data and numerical results obtained from Pitot tube and hot-film anemometer measurements. Explanation of the symbols used is as follows:

SYMBOL	EXPLANATION
Y	Radial position (y) from the pipe wall.
TEM	Temperature of the fluid (°C).
DELTA-PSI	Local pressure drop measured with the Pitot tube (psi).
FT/SC	Local fluid velocity (ft/sec).
DIMR	Dimensionless radius (y/R).
DIMU	Dimensionless velocity defined as the ratio of the local velocity at a given radial position (y) to the tube axis velocity.
DIMUC	Dimensionless velocity defined as the ratio of the local velocity at a given radial position (y) to the average bulk velocity obtained from calibration.
U^+	Dimensionless velocity (u^+) defined by equation 11.
Y^+	Dimensionless distance (y^+) defined by equation 11.

PITOT TUBE MEASUREMENTS

RUN= 1 TOLUENE

Y	TEM	DELTA-PSI	FT/SC	DIMR	DIMU	DIMUC	U+	Y+
0.500	24.900	0.220	6.161	1.000	1.000	1.253	24.676	1478.350
0.418	24.900	0.214	6.075	0.836	0.986	1.236	24.331	1182.679
0.318	24.900	0.199	5.863	0.636	0.951	1.192	23.482	887.010
0.268	24.900	0.186	5.661	0.536	0.918	1.151	22.676	739.170
0.218	24.900	0.175	5.491	0.436	0.891	1.117	21.994	591.340
0.168	24.900	0.164	5.316	0.336	0.862	1.081	21.291	443.500
0.118	24.900	0.144	4.988	0.236	0.809	1.014	19.980	295.670
0.068	24.900	0.125	4.638	0.136	0.752	0.943	18.576	147.830
0.048	24.900	0.113	4.405	0.096	0.714	0.896	17.642	88.700
0.028	24.900	0.097	4.082	0.056	0.662	0.830	16.348	29.560

CALIBRATED AVERAGE VELOCITY= 4.917 FRICTION FACTOR= 0.00515000

INTEGRATED AVERAGE VELOCITY= 5.113 REYNOLDS NUMBER= 58212.600

FLOW RATE (POUNDS/MINUTE) = 86.500

PITOT TUBE MEASUREMENTS

RUN= 2 TOLUENE

Y	TEM	DELTA-PSI	FT/SC	DIMR	DIMU	DIMUC	U+	Y+
0.500	24.900	0.647	10.561	1.000	1.000	1.202	25.785	2425.139
0.418	24.900	0.634	10.451	0.836	0.989	1.190	25.516	1940.110
0.318	24.900	0.590	10.081	0.636	0.954	1.148	24.613	1455.080
0.268	24.900	0.563	9.848	0.536	0.932	1.121	24.045	1212.570
0.218	24.900	0.530	9.555	0.436	0.904	1.088	23.329	970.050
0.168	24.900	0.493	9.218	0.336	0.872	1.050	22.506	727.540
0.118	24.900	0.447	8.773	0.236	0.830	0.999	21.419	485.030
0.068	24.900	0.379	8.085	0.136	0.765	0.921	19.739	242.510
0.048	24.900	0.349	7.752	0.096	0.734	0.883	18.926	145.510
0.028	24.900	0.295	7.128	0.056	0.674	0.812	17.404	48.500

CALIBRATED AVERAGE VELOCITY= 8.783

INTEGRATED AVERAGE VELOCITY= 8.892

FLOW RATE (POUNDS/MINUTE) = 154.500

FRICTION FACTOR= 0.00434000

REYNOLDS NUMBER= 103975.100

PITOT TUBE MEASUREMENTS

RUN= 3 TOLUENE

Y	TEM	DELTA-PSI	FT/SC	DIMR	DIMU	DIMUC	U+	Y+
0.500	25.000	1.308	15.017	1.000	1.000	1.204	26.565	3346.669
0.418	25.300	1.295	14.939	0.836	0.987	1.198	26.427	2676.479
0.318	25.300	1.199	14.378	0.636	0.962	1.153	25.435	2007.360
0.268	25.300	1.136	13.992	0.536	0.936	1.122	24.752	1672.790
0.218	25.300	1.071	13.594	0.436	0.909	1.090	24.048	1338.229
0.168	25.300	0.992	13.080	0.336	0.875	1.049	23.139	1003.679
0.118	25.300	0.913	12.546	0.236	0.839	1.006	22.193	669.120
0.068	25.300	0.794	11.702	0.136	0.783	0.938	20.701	334.560
0.048	25.300	0.728	11.205	0.096	0.750	0.898	19.822	200.740
0.028	25.300	0.619	10.333	0.056	0.691	0.828	18.280	66.910

CALIBRATED AVERAGE VELOCITY= 12.474 FRICTION FACTOR= 0.00410000

INTEGRATED AVERAGE VELOCITY= 12.720 REYNOLDS NUMBER= 147651.300

FLOW RATE (POUNDS/MINUTE) = 219.400

PITOT TUBE MEASUREMENTS

RUN= 4 TOLUENE

Y	TEM	DELTA-PSI	FT/SC	DIMR	DIMU	DIMUC	U+	Y+
0.500	25.000	2.149	19.245	1.000	1.000	1.192	26.884	4238.109
0.418	25.000	2.119	19.113	0.836	0.993	1.184	26.699	3390.489
0.318	25.000	1.998	18.560	0.636	0.964	1.149	25.926	2542.870
0.268	25.000	1.908	18.135	0.536	0.942	1.123	25.332	2119.050
0.218	25.000	1.796	17.598	0.436	0.914	1.090	24.583	1695.239
0.168	25.300	1.688	17.062	0.336	0.886	1.057	23.834	1271.030
0.118	25.300	1.535	16.272	0.236	0.845	1.008	22.730	847.350
0.068	25.300	1.341	15.207	0.136	0.790	0.942	21.243	423.670
0.048	25.300	1.226	14.541	0.096	0.755	0.901	20.312	254.210
0.028	25.300	1.039	13.386	0.056	0.695	0.829	18.699	84.730

CALIBRATED AVERAGE VELOCITY= 16.147 FRICTION FACTOR= 0.00393000

INTEGRATED AVERAGE VELOCITY= 16.470 REYNOLDS NUMBER= 191125.800

FLOW RATE (POUNDS/MINUTE) = 284.000

PITOT TUBE MEASUREMENTS

RUN= 5 TOLUENE

Y	TEM	DELTA-PSI	FT/SC	DIMR	DIMU	DIMUC	U+	Y+
0.500	25.200	2.868	22.238	1.000	1.000	1.193	27.402	4803.511
0.418	25.200	2.778	21.884	0.836	0.984	1.174	26.966	3842.510
0.318	25.200	2.615	21.234	0.636	0.954	1.139	26.144	2882.100
0.268	25.200	2.506	20.788	0.536	0.934	1.115	25.616	2401.750
0.218	25.200	2.362	20.179	0.436	0.907	1.082	24.865	1921.399
0.168	25.200	2.199	19.472	0.336	0.875	1.044	23.993	1441.050
0.118	25.200	2.036	18.737	0.236	0.842	1.005	23.088	960.700
0.068	25.200	1.783	17.533	0.136	0.788	0.940	21.605	480.350
0.048	25.200	1.620	16.714	0.096	0.751	0.896	20.595	288.210
0.028	25.200	1.367	15.353	0.056	0.690	0.823	18.918	96.070

CALIBRATED AVERAGE VELOCITY= 18.648 FRICTION FACTOR= 0.00378000

INTEGRATED AVERAGE VELOCITY= 18.892 REYNOLDS NUMBER= 220736.800

FLOW RATE (POUNDS/MINUTE) = 328.000

PITOT TUBE MEASUREMENTS

RUN= 6 ALUMINIUM DIOLEATE (1%) IN TOLUENE

Y	TEM	DELTA-PSI	FT/SC	DIMR	DIMU	DIMUC	U+	Y+
0.500	25.000	0.483	9.128	1.000	1.000	1.036	26.342	824.723
0.468	25.000	0.481	9.105	0.936	0.997	1.033	26.275	742.253
0.418	25.000	0.471	9.012	0.836	0.987	1.023	26.007	659.786
0.368	25.000	0.457	8.882	0.736	0.973	1.008	25.632	577.304
0.318	25.000	0.446	8.775	0.636	0.961	0.996	25.322	494.834
0.268	25.000	0.422	8.531	0.536	0.934	0.968	24.619	412.359
0.218	25.000	0.413	8.444	0.436	0.925	0.958	24.368	329.889
0.168	25.000	0.392	8.229	0.336	0.901	0.934	23.747	247.415
0.118	25.000	0.361	7.889	0.236	0.864	0.895	22.766	164.945
0.068	25.000	0.299	7.189	0.136	0.787	0.816	20.748	82.470
0.048	25.000	0.265	6.766	0.096	0.741	0.768	19.527	49.482
0.028	25.000	0.209	6.007	0.056	0.658	0.682	17.335	16.494

CALIBRATED AVERAGE VELOCITY= 8.812 FRICTION FACTOR= 0.00309000

INTEGRATED AVERAGE VELOCITY= 7.826 REYNOLDS NUMBER= 103975.000

FLOW RATE (POUNDS/MINUTE) = 155.000

PITOT TUBE MEASUREMENTS

RUN= 7 ALUMINIUM DIOLEATE (1%) IN TOLUENE

Y	TEM	DELTA-PSI	FT/SC	DIMR	DIMU	DIMUC	U+	Y+
0.500	25.000	1.001	13.140	1.000	1.000	1.027	30.070	1039.989
0.468	25.000	0.999	13.124	0.936	0.998	1.026	30.033	935.993
0.418	25.000	0.984	13.027	0.836	0.991	1.018	29.811	831.991
0.368	25.000	0.963	12.889	0.736	0.980	1.008	29.495	727.994
0.318	25.000	0.938	12.716	0.636	0.967	0.994	29.099	623.996
0.268	25.000	0.901	12.464	0.536	0.948	0.974	28.524	519.995
0.218	25.000	0.857	12.156	0.436	0.925	0.950	27.818	415.998
0.168	25.000	0.806	11.786	0.336	0.896	0.921	26.972	311.996
0.118	25.000	0.744	11.330	0.236	0.862	0.886	25.928	207.999
0.068	25.000	0.640	10.508	0.136	0.799	0.821	24.048	103.997
0.048	25.000	0.584	10.036	0.096	0.763	0.785	22.968	62.398
0.028	25.000	0.470	9.006	0.056	0.685	0.704	20.611	20.799

CALIBRATED AVERAGE VELOCITY= 12.792 FRICTION FACTOR= 0.00233000

INTEGRATED AVERAGE VELOCITY= 11.350 REYNOLDS NUMBER= 147651.000

FLOW RATE (POUNDS/MINUTE) = 225.000

PITOT TUBE MEASUREMENTS

RUN= 8 ALUMINIUM DIOLEATE (1%) IN TOLUENE

Y	TEM	DELTA-PSI	FT/SC	DIMR	DIMU	DIMUC	U+	Y+
0.500	25.400	1.573	16.471	1.000	1.000	1.053	32.349	1211.258
0.468	25.400	1.566	16.432	0.936	0.997	1.051	32.273	1090.131
0.418	25.400	1.552	16.361	0.836	0.993	1.046	32.133	969.005
0.368	25.400	1.518	16.179	0.736	0.982	1.034	31.776	847.878
0.318	25.400	1.472	15.935	0.636	0.967	1.019	31.297	726.752
0.268	25.400	1.432	15.714	0.536	0.954	1.005	30.863	605.629
0.218	25.400	1.378	15.415	0.436	0.935	0.985	30.276	484.502
0.168	25.400	1.295	14.948	0.336	0.907	0.956	29.359	363.376
0.118	25.400	1.183	14.282	0.236	0.867	0.913	28.050	242.249
0.068	25.400	1.025	13.300	0.136	0.807	0.850	26.121	121.123
0.048	25.400	0.892	12.402	0.096	0.753	0.793	24.358	72.674
0.028	25.400	0.615	10.305	0.056	0.625	0.659	20.240	24.220

CALIBRATED AVERAGE VELOCITY= 15.642 FRICTION FACTOR= 0.00212000

INTEGRATED AVERAGE VELOCITY= 14.242 REYNOLDS NUMBER= 185069.000

FLOW RATE (POUNDS/MINUTE) = 275.000

PITOT TUBE MEASUREMENTS

RUN= 9 ALUMINIUM DIOLEATE (1%) IN TOLUENE

Y	TFM	DELTA-PSI	FT/SC	DIMR	DIMU	DIMUC	U+	Y+
0.500	25.000	2.317	19.985	1.000	1.000	1.056	34.524	1377.706
0.468	25.000	2.296	19.895	0.936	0.995	1.051	34.368	1239.932
0.418	24.800	2.271	19.784	0.836	0.989	1.045	34.175	1102.633
0.368	24.800	2.226	19.584	0.736	0.979	1.034	33.831	964.804
0.318	24.800	2.164	19.311	0.636	0.966	1.020	33.360	826.974
0.268	24.800	2.099	19.018	0.536	0.951	1.004	32.853	689.145
0.218	24.800	2.018	18.646	0.436	0.933	0.985	32.211	551.315
0.168	24.800	1.898	18.088	0.336	0.905	0.955	31.247	413.397
0.118	24.800	1.748	17.358	0.236	0.868	0.917	29.985	275.595
0.068	24.800	1.531	16.246	0.136	0.812	0.858	28.065	137.798
0.048	24.800	1.407	15.573	0.096	0.779	0.823	26.902	82.679
0.028	24.800	1.094	13.734	0.056	0.687	0.725	23.725	27.557

CALIBRATED AVERAGE VELOCITY= 18.933 FRICTION FACTOR= 0.00186000

INTEGRATED AVERAGE VELOCITY= 17.384 REYNOLDS NUMBER= 224101.600

FLOW RATE (POUNDS/MINUTE) = 333.000

PITOT TUBE MEASUREMENTS

RUN= 10 CYCLOHEXANE

Y	TEM	DELTA-PSI	FT/SC	DIMR	DIMU	DIMUC	U+	Y+
0.500	25.500	0.259	7.048	1.000	1.000	1.170	21.917	1084.689
0.418	25.500	0.254	6.988	0.836	0.991	1.160	21.731	867.750
0.318	25.500	0.239	6.774	0.636	0.961	1.125	21.066	650.810
0.268	25.500	0.226	6.585	0.536	0.934	1.093	20.478	542.340
0.218	25.500	0.213	6.391	0.436	0.906	1.061	19.874	325.400
0.168	25.500	0.197	6.156	0.336	0.873	1.022	19.144	433.870
0.118	25.500	0.181	5.895	0.236	0.836	0.979	18.331	216.930
0.068	25.500	0.163	5.602	0.136	0.794	0.930	17.421	108.460
0.048	25.500	0.151	5.392	0.096	0.765	0.895	16.767	65.080
0.028	25.500	0.123	4.858	0.056	0.689	0.807	15.108	21.690

CALIBRATED AVERAGE VELOCITY= 6.023 FRICTION FACTOR= 0.00570000

INTEGRATED AVERAGE VELOCITY= 5.986 REYNOLDS NUMBER= 40619.890

FLOW RATE (POUNDS/MINUTE) = 95.330

PITOT TUBE MEASUREMENTS

RUN= 11 CYCLOHEXANE

Y	TEM	DELTA-PSI	FT/SC	DIMR	DIMU	DIMUC	U+	Y+
0.500	25.600	0.665	11.290	1.000	1.000	1.207	24.415	1559.530
0.418	25.600	0.646	11.131	0.836	0.985	1.190	24.070	1247.629
0.318	25.600	0.596	10.688	0.636	0.946	1.143	23.112	935:720
0.268	25.600	0.564	10.399	0.536	0.921	1.112	22.487	779.760
0.218	25.600	0.529	10.070	0.436	0.891	1.077	21.777	623.810
0.168	25.600	0.469	9.479	0.336	0.839	1.014	20.498	467.860
0.118	25.600	0.413	8.895	0.236	0.787	0.951	19.237	311.900
0.068	25.600	0.368	8.397	0.136	0.743	0.898	18.159	155.950
0.048	25.600	0.330	7.960	0.096	0.705	0.851	17.214	93.570
0.028	25.600	0.282	7.357	0.056	0.651	0.787	15.909	31.190

CALIBRATED AVERAGE VELOCITY= 9.352 FRICTION FACTOR= 0.00489000

INTEGRATED AVERAGE VELOCITY= 9.261 REYNOLDS NUMBER= 63052.000

FLOW RATE (POUNDS/MINUTE) = 148.000

132041

PITOT TUBE MEASUREMENTS

RUN= 12 CYCLOHEXANE

Y	TEM	DELTA-PSI	FT/SC	DIMR	DIMU	DIMUC	U+	Y+
0.500	25.500	1.178	15.022	1.000	1.000	1.217	24.972	2029.229
0.418	25.500	1.146	14.818	0.836	0.986	1.200	24.632	1623.379
0.318	25.500	1.064	14.277	0.636	0.950	1.156	23.733	1217.530
0.268	25.500	1.009	13.904	0.536	0.925	1.126	23.113	1014.610
0.218	25.500	0.887	13.039	0.436	0.867	1.056	21.675	811.610
0.168	25.500	0.869	12.901	0.336	0.858	1.045	21.446	608.770
0.118	25.500	0.785	12.267	0.236	0.816	0.994	20.392	405.840
0.068	25.500	0.667	11.305	0.136	0.752	0.916	18.793	202.920
0.048	25.500	0.607	10.782	0.096	0.717	0.873	17.924	121.750
0.028	25.500	0.509	9.878	0.056	0.657	0.800	16.420	40.580

CALIBRATED AVERAGE VELOCITY= 12.345 FRICTION FACTOR= 0.00474000

INTEGRATED AVERAGE VELOCITY= 12.439 REYNOLDS NUMBER= 83259.500

FLOW RATE (POUNDS/MINUTE) = 195.400

PITOT TUBE MEASUREMENTS

RUN= 13 CYCLOHEXANE

Y	TEM	DELTA-PSI	FT/SC	DIMR	DIMU	DIMUC	U+	Y+
0.500	25.500	1.826	18.704	1.000	1.000	1.222	25.486	2475.000
0.418	25.500	1.780	18.467	0.836	0.987	1.207	25.163	1980.000
0.318	25.500	1.658	17.824	0.636	0.952	1.165	24.288	1485.000
0.268	25.500	1.570	17.347	0.536	0.927	1.133	23.637	1237.000
0.218	25.500	1.477	16.824	0.436	0.899	1.099	22.925	990.000
0.168	25.500	1.369	16.194	0.336	0.865	1.058	22.067	742.500
0.118	25.500	1.232	15.362	0.236	0.821	1.004	20.933	495.000
0.068	25.500	1.057	14.234	0.136	0.761	0.930	19.395	247.500
0.048	25.500	1.001	13.853	0.096	0.740	0.905	18.876	148.500
0.028	25.500	0.813	12.481	0.056	0.667	0.815	17.006	49.500

CALIBRATED AVERAGE VELOCITY= 15.305 FRICTION FACTOR= 0.00459000

INTEGRATED AVERAGE VELOCITY= 15.664 REYNOLDS NUMBER= 103200.000

FLOW RATE (POUNDS/MINUTE) = 242.000

TOT

PITOT TUBE MEASUREMENTS

RUN= 14 CYCLOHEXANE

Y	TEM	DELTA-PSI	FT/SC	DIMR	DIMU	DIMUC	U+	Y+
0.500	25.200	2.630	22.456	1.000	1.000	1.224	26.263	2881.219
0.418	25.200	2.557	22.143	0.836	0.986	1.207	25.897	2304.979
0.318	25.200	2.375	21.340	0.636	0.950	1.164	24.958	1728.729
0.268	25.200	2.266	20.843	0.536	0.928	1.136	24.377	1440.610
0.218	25.200	2.120	20.162	0.436	0.897	1.099	23.580	1152.489
0.168	25.200	1.938	19.277	0.336	0.858	1.051	22.545	864.370
0.118	25.200	1.792	18.538	0.236	0.825	1.011	21.681	576.240
0.068	25.200	1.537	17.169	0.136	0.764	0.936	20.080	288.120
0.048	25.200	1.373	16.228	0.096	0.722	0.885	18.979	172.870
0.028	25.200	1.136	14.763	0.056	0.657	0.805	17.266	57.620

CALIBRATED AVERAGE VELOCITY= 18.341 FRICTION FACTOR= 0.00434000

INTEGRATED AVERAGE VELOCITY= 18.752 REYNOLDS NUMBER= 123568.000

FLOW RATE (POUNDS/MINUTE) = 290.000

PITOT TUBE MEASUREMENTS

RUN= 15 POLYISOBUTYLENE (0.2%) IN CYCLOHEXANE

Y	TEM	DELTA-PSI	FT/SC	DIMR	DIMU	DIMUC	U+	Y+
0.500	25.700	0.241	6.797	1.000	1.000	1.128	21.745	693.236
0.400	25.700	0.236	6.719	0.800	0.988	1.115	21.495	554.589
0.300	25.700	0.217	6.446	0.600	0.948	1.070	20.623	415.941
0.200	25.700	0.189	6.022	0.400	0.886	0.999	19.268	277.294
0.150	25.700	0.173	5.753	0.300	0.846	0.955	18.407	207.968
0.100	25.700	0.155	5.452	0.200	0.802	0.905	17.442	138.647
0.050	25.700	0.128	4.944	0.100	0.727	0.820	15.817	69.320
0.021	25.700	0.086	4.051	0.042	0.596	0.672	12.962	29.110

CALIBRATED AVERAGE VELOCITY= 6.026 FRICTION FACTOR= 0.00538000

INTEGRATED AVERAGE VELOCITY= 5.422 REYNOLDS NUMBER= 40619.890

FLOW RATE (POUNDS/MINUTE) = 95.330

PITOT TUBE MEASUREMENTS

RUN= 16 POLYISOBUTYLENE (0.2%) IN CYCLOHEXANE

Y	TEM	DELTA-PSI	FT/SC	DIMR	DIMU	DIMUC	U+	Y+
0.500	26.100	0.469	9.482	1.000	1.000	1.049	20.794	1010.898
0.400	26.100	0.459	9.382	0.800	0.989	1.037	20.573	808.715
0.300	26.100	0.426	9.037	0.600	0.953	0.999	19.819	606.544
0.200	26.100	0.374	8.470	0.400	0.893	0.937	18.575	404.361
0.150	26.100	0.344	8.119	0.300	0.856	0.898	17.804	303.614
0.100	26.100	0.303	7.623	0.200	0.804	0.843	16.718	202.407
0.050	26.300	0.261	7.064	0.100	0.745	0.781	15.491	101.207
0.021	26.500	0.200	6.189	0.042	0.652	0.684	13.572	42.507

CALIBRATED AVERAGE VELOCITY= 9.043 FRICTION FACTOR= 0.00372000

INTEGRATED AVERAGE VELOCITY= 7.675 REYNOLDS NUMBER= 63052.000

FLOW RATE (POUNDS/MINUTE) = 143.000

PITOT TUBE MEASUREMENTS

RUN= 17 POLYISOBUTYLENE (0.2%) IN CYCLOHEXANE

Y	TEM	DELTA-PSI	FT/SC	DIMR	DIMU	DIMUC	U+	Y+
0.500	25.800	0.721	11.758	1.000	1.000	0.954	22.979	1134.687
0.400	25.800	0.715	11.704	0.800	0.995	0.949	22.873	907.750
0.300	25.800	0.675	11.374	0.600	0.967	0.922	22.230	680.813
0.200	25.800	0.597	10.694	0.400	0.909	0.867	20.899	453.875
0.150	25.900	0.561	10.373	0.300	0.882	0.841	20.272	340.403
0.100	25.900	0.497	9.764	0.200	0.830	0.792	19.082	226.938
0.050	25.900	0.419	8.962	0.100	0.762	0.727	17.516	113.466
0.021	25.900	0.328	7.923	0.042	0.673	0.643	15.485	47.652

CALIBRATED AVERAGE VELOCITY= 12.331 FRICTION FACTOR= 0.00344000

INTEGRATED AVERAGE VELOCITY= 9.722 REYNOLDS NUMBER= 83259.500

FLOW RATE (POUNDS/MINUTE) = 195.000

PITOT TUBE MEASUREMENTS

RUN= 18 POLYISOBUTYLENE (0.4%) IN CYCLOHEXANE

Y	TEM	DELTA-PSI	FT/SC	DIMR	DIMU	DIMUC	U+	Y+
0.500	24.710	0.496	9.744	1.000	1.000	0.791	18.670	410.332
0.400	24.710	0.485	9.635	0.800	0.988	0.782	18.461	328.264
0.300	24.750	0.463	9.412	0.600	0.966	0.764	18.035	246.197
0.200	24.730	0.430	9.068	0.400	0.930	0.736	17.376	164.132
0.150	24.750	0.393	8.674	0.300	0.890	0.704	16.621	123.099
0.100	24.750	0.369	8.401	0.200	0.862	0.682	16.097	82.065
0.050	24.750	0.324	7.880	0.100	0.808	0.640	15.100	41.031
0.021	24.750	0.225	6.560	0.042	0.673	0.533	12.570	17.233

CALIBRATED AVERAGE VELOCITY= 12.315 FRICTION FACTOR= 0.00359000

INTEGRATED AVERAGE VELOCITY= 8.216 REYNOLDS NUMBER= 83259.500

FLOW RATE (POUNDS/MINUTE) = 195.000

PITOT TUBE MEASUREMENTS

RUN= 19 POLYISOBUTYLENE (0.4%) IN CYCLOHEXANE

Y	TEM	DELTA-PSI	FT/SC	DIMR	DIMU	DIMUC	U+	Y+
0.500	24.300	0.197	6.139	1.000	1.000	1.020	18.068	267.249
0.400	24.300	0.187	5.981	0.800	0.974	0.994	17.606	213.798
0.300	24.300	0.174	5.765	0.600	0.939	0.958	16.969	160.348
0.200	24.300	0.153	5.405	0.400	0.880	0.898	15.909	106.898
0.150	24.300	0.139	5.164	0.300	0.841	0.858	15.201	80.173
0.100	24.340	0.125	4.891	0.200	0.796	0.813	14.395	69.758
0.050	24.340	0.107	4.531	0.100	0.738	0.753	13.337	26.723
0.021	24.350	0.067	3.593	0.042	0.585	0.597	10.575	11.224

CALIBRATED AVERAGE VELOCITY= 6.018 FRICTION FACTOR= 0.00537000

INTEGRATED AVERAGE VELOCITY= 4.868 REYNOLDS NUMBER= 40619.890

FLOW RATE (POUNDS/MINUTE) = 95.330

PITOT TUBE MEASUREMENTS

RUN= 20 POLYISOBUTYLENE (0.4%) IN CYCLOHEXANE

Y	TEM	DELTA-PSI	FT/SC	DIMR	DIMU	DIMUC	U+	Y+
0.500	24.100	0.343	8.102	1.000	1.000	0.898	17.804	358.032
0.400	24.100	0.332	7.970	0.800	0.983	0.883	17.515	286.494
0.300	24.100	0.314	7.755	0.600	0.957	0.859	17.042	214.819
0.200	24.100	0.284	7.377	0.400	0.910	0.817	16.211	143.211
0.150	24.100	0.263	7.099	0.300	0.876	0.787	15.602	107.408
0.100	24.100	0.239	6.763	0.200	0.834	0.749	14.863	71.606
0.050	24.150	0.201	6.208	0.100	0.766	0.688	13.643	35.803
0.021	24.150	0.051	3.123	0.042	0.385	0.346	6.863	15.035

CALIBRATED AVERAGE VELOCITY= 9.025 FRICTION FACTOR= 0.00372000

INTEGRATED AVERAGE VELOCITY= 6.464 REYNOLDS NUMBER= 63052.000

FLOW RATE (POUNDS/MINUTE) = 143.000

HOT-FILM ANEMOMETER MEASUREMENTS

RUN= 21 ALUMINIUM DIOLEATE (1%) IN TOLUENE

Y	TEM	VOLTAGE	FT/SC	DIMR	DIMU	DIMUC	U+	Y+
0.500	26.500	21.410	10.750	1.000	1.000	1.218	31.341	820.546
0.450	26.500	21.410	10.750	0.900	1.000	1.218	31.341	738.491
0.400	26.500	21.370	10.700	0.800	0.995	1.212	31.195	656.437
0.350	26.500	21.350	10.680	0.700	0.993	1.210	31.136	574.382
0.300	26.500	21.330	10.640	0.600	0.990	1.205	31.020	492.327
0.250	26.500	21.280	10.580	0.500	0.984	1.199	30.845	410.273
0.200	26.500	21.100	10.330	0.400	0.961	1.170	30.116	328.218
0.150	26.500	20.790	9.920	0.300	0.923	1.124	28.921	246.164
0.100	26.500	20.170	9.130	0.200	0.849	1.034	26.618	164.109
0.050	26.500	19.130	7.900	0.100	0.735	0.895	23.032	82.055
0.040	26.500	18.440	7.160	0.080	0.666	0.811	20.874	65.644

CALIBRATED AVERAGE VELOCITY= 8.827 FRICTION FACTOR= 0.00302000

INTEGRATED AVERAGE VELOCITY= 8.673 REYNOLDS NUMBER= 103975.000

FLOW RATE (POINDS/MINUTE) = 155.000

HOT-FILM ANEMOMETER MEASUREMENTS

RUN= 22 ALUMINIUM DIOLEATE (1%) IN TOLUENE

Y	TEM	VOLTAGE	FT/SC	DIMR	DIMU	DIMUC	U+	Y+
0.500	26.500	25.490	15.610	1.000	1.000	1.249	36.277	1029.367
0.450	26.500	25.220	15.590	0.900	0.999	1.247	36.231	926.431
0.400	26.500	25.120	15.400	0.800	0.987	1.232	35.789	823.494
0.350	26.500	25.090	15.390	0.700	0.986	1.231	35.766	720.558
0.300	26.500	24.970	15.120	0.600	0.969	1.210	35.138	617.621
0.250	26.500	24.840	15.000	0.500	0.961	1.200	34.860	514.684
0.200	26.500	24.550	14.500	0.400	0.929	1.160	33.698	411.747
0.150	26.500	24.320	14.100	0.300	0.903	1.128	32.768	308.810
0.100	26.500	23.880	13.410	0.200	0.859	1.073	31.164	205.874
0.050	26.500	22.270	11.090	0.100	0.710	0.887	25.773	102.937
0.040	26.500	20.480	8.800	0.080	0.564	0.704	20.451	82.349

CALIBRATED AVERAGE VELOCITY= 12.500 FRICTION FACTOR= 0.00237000

INTEGRATED AVERAGE VELOCITY= 12.641 REYNOLDS NUMBER= 151420.000

FLOW RATE (POUNDS/MINUTE) = 219.500

HOT-FILM ANEMOMETER MEASUREMENTS

RUN= 23 CYCLOHEXANE

Y	TEM	VOLTAGE	FT/SC	DIMR	DIMU	DIMUC	U+	Y+
0.500	26.800	18.650	7.320	1.000	1.000	1.217	22.796	1083.220
0.450	26.800	18.640	7.300	0.900	0.997	1.214	22.733	974.898
0.400	26.800	18.630	7.280	0.800	0.995	1.210	22.671	866.576
0.350	26.800	18.570	7.160	0.700	0.978	1.190	22.297	758.255
0.300	26.800	18.500	7.020	0.600	0.959	1.167	21.861	649.933
0.250	26.800	18.390	6.820	0.500	0.932	1.134	21.239	541.611
0.200	26.800	18.300	6.630	0.400	0.906	1.102	20.647	433.288
0.150	26.800	18.190	6.420	0.300	0.877	1.067	19.993	324.966
0.100	26.800	17.850	5.820	0.200	0.795	0.968	18.124	216.644
0.050	26.800	17.410	5.090	0.100	0.695	0.846	15.851	108.322
0.018	26.800	16.800	4.200	0.036	0.574	0.698	13.080	38.996

CALIBRATED AVERAGE VELOCITY= 6.015 FRICTION FACTOR= 0.00570000

INTEGRATED AVERAGE VELOCITY= 5.901 REYNOLDS NUMBER= 40619.800

FLOW RATE (POUNDS/MINUTE) = 95.000

HOT-FILM ANEMOMETER MEASUREMENTS

RUN= 24 CYCLOHEXANE

Y	TEM	VOLTAGE	FT/SC	DIMR	DIMU	DIMUC	U+	Y+
0.500	24.900	21.300	11.010	1.000	1.000	1.215	24.189	1535.400
0.400	24.900	21.290	10.650	0.800	0.967	1.176	23.398	1228.321
0.300	24.900	21.210	10.500	0.600	0.954	1.159	23.069	921.240
0.200	24.900	21.100	10.100	0.400	0.917	1.115	22.190	614.160
0.150	24.900	20.860	9.200	0.300	0.836	1.016	20.213	460.620
0.100	24.900	20.540	8.900	0.200	0.808	0.983	19.554	307.080
0.050	24.900	19.980	7.700	0.100	0.699	0.850	16.917	153.540
0.020	24.900	19.630	7.040	0.040	0.639	0.777	15.467	61.416

CALIBRATED AVERAGE VELOCITY= 9.058 FRICTION FACTOR= 0.00505000

INTEGRATED AVERAGE VELOCITY= 8.844 REYNOLDS NUMBER= 60932.000

FLOW RATE (POINDS/MINUTE) = 143.000

HOT-FILM ANEMOMETER MEASUREMENTS

RUN= 25 CYCLOHEXANE

Y	TEM	VOLTAGE	FT/SC	DIMR	DIMU	DIMUC	U+	Y+
0.500	24.900	21.840	15.000	1.000	1.000	1.215	24.959	2027.329
0.400	24.900	21.780	14.520	0.800	0.968	1.176	24.160	1621.863
0.300	24.900	21.650	14.100	0.600	0.940	1.142	23.461	1216.396
0.200	24.900	21.300	13.020	0.400	0.868	1.055	21.664	810.931
0.150	24.900	21.210	12.850	0.300	0.857	1.041	21.381	608.198
0.100	24.900	20.930	12.050	0.200	0.803	0.976	20.050	405.466
0.050	24.900	20.560	10.920	0.100	0.728	0.885	18.170	202.733
0.020	24.900	20.150	9.900	0.040	0.660	0.802	16.473	81.093

CALIBRATED AVERAGE VELOCITY= 12.345 FRICTION FACTOR= 0.00474000

INTEGRATED AVERAGE VELOCITY= 12.017 REYNOLDS NUMBER= 83259.500

FLOW RATE (POINDS/MINUTE) = 196.000

HOT-FILM ANEMOMETER MEASUREMENTS

RUN= 26 POLYISOBUTYLENE (0.2%) IN CYCLOHEXANE

Y	TEM	VOLTAGE	FT/SC	DIMR	DIMU	DIMUC	U+	Y+
0.500	27.170	17.290	7.985	1.000	1.000	1.327	25.587	693.395
0.400	27.170	17.180	7.582	0.800	0.950	1.260	24.296	554.716
0.300	27.170	17.060	7.129	0.600	0.893	1.185	22.844	416.037
0.200	27.170	16.860	6.341	0.400	0.794	1.054	20.319	277.358
0.150	27.170	16.840	6.259	0.300	0.784	1.040	20.056	208.019
0.100	27.170	16.740	5.843	0.200	0.732	0.971	18.723	138.679
0.050	27.170	16.620	5.323	0.100	0.667	0.885	17.057	69.340
0.018	27.170	16.330	3.931	0.036	0.492	0.653	12.596	24.962

CALIBRATED AVERAGE VELOCITY= 6.017 FRICTION FACTOR= 0.00538000

INTEGRATED AVERAGE VELOCITY= 5.860 REYNOLDS NUMBER= 40619.800

FLOW RATE (POINDS/MINUTE) = 95.330

HOT-FILM ANEMOMETER MEASUREMENTS

RUN= 27 POLYISOBUTYLENE (0.2%) IN CYCLOHEXANE

Y	TEM	VOLTAGE	FT/SC	DIMR	DIMU	DIMUC	U+	Y+
0.500	27.100	13.320	11.080	1.000	1.000	1.228	28.467	864.825
0.400	27.100	13.250	10.720	0.800	0.968	1.188	27.542	691.860
0.300	27.100	13.180	10.350	0.600	0.934	1.147	26.591	518.895
0.200	27.100	12.960	9.100	0.400	0.821	1.008	23.380	345.930
0.150	27.100	12.850	8.400	0.300	0.758	0.931	21.581	259.447
0.100	27.100	12.820	8.300	0.200	0.749	0.920	21.324	172.965
0.050	27.100	12.740	7.900	0.100	0.713	0.875	20.297	86.482
0.018	27.100	12.620	7.300	0.036	0.659	0.809	18.755	31.134

CALIBRATED AVERAGE VELOCITY= 9.025 FRICTION FACTOR= 0.00372000

INTEGRATED AVERAGE VELOCITY= 8.781 REYNOLDS NUMBER= 60932.000

FLOW RATE (POINDS/MINUTE) = 143.000

HOT-FILM ANEMOMETER MEASUREMENTS

RUN= 28 POLYISOBUTYLENE (0.2%) IN CYCLOHEXANE

Y	TEM	VOLTAGE	FT/SC	DIMR	DIMU	DIMUC	U+	Y+
0.500	27.700	21.050	15.000	1.000	1.000	1.209	29.144	1143.564
0.400	27.700	20.930	14.460	0.800	0.964	1.165	28.095	914.851
0.300	27.700	20.850	14.118	0.600	0.941	1.138	27.431	686.138
0.200	27.700	20.730	13.618	0.400	0.908	1.097	26.459	457.425
0.150	27.700	20.620	13.170	0.300	0.878	1.061	25.589	343.069
0.100	27.700	20.500	12.693	0.200	0.846	1.023	24.662	228.713
0.050	27.700	20.300	11.923	0.100	0.795	0.961	23.166	114.356
0.018	27.700	20.080	11.111	0.036	0.741	0.895	21.588	41.168

CALIBRATED AVERAGE VELOCITY= 12.410 FRICTION FACTOR= 0.00344000

INTEGRATED AVERAGE VELOCITY= 12.391 REYNOLDS NUMBER= 83259.000

FLOW RATE (POINDS/MINUTE) = 196.000

RUN= 29 POLYISOBUTYLENE (0.4%) IN CYCLOHEXANE

Y	TEM	VOLTAGE	FT/SC	DIMR	DIMU	DIMUC	U+	Y+
0.500	22.400	19.860	8.600	1.000	1.000	1.429	27.579	246.149
0.400	22.400	19.700	8.300	0.800	0.965	1.379	26.617	196.919
0.300	22.400	19.380	7.600	0.600	0.884	1.263	24.372	147.690
0.200	22.400	18.850	6.500	0.400	0.756	1.080	20.844	98.460
0.150	22.400	18.280	5.700	0.300	0.663	0.947	18.279	73.845
0.100	22.400	18.080	5.400	0.200	0.628	0.897	17.317	49.230
0.050	22.400	17.840	5.050	0.100	0.587	0.839	16.194	24.615
0.020	22.400	17.300	4.100	0.040	0.477	0.681	13.148	9.846

CALIBRATED AVERAGE VELOCITY= 6.018 FRICTION FACTOR= 0.00537000

INTEGRATED AVERAGE VELOCITY= 5.830 REYNOLDS NUMBER= 40619.800

FLOW RATE (POINDS/MINUTE) = 95.330

HOT-FILM ANEMOMETER MEASUREMENTS

RUN= 30 POLYISOBUTYLENE (0.4%) IN CYCLOHEXANE

Y	TEM	VOLTAGE	FT/SC	DIMR	DIMU	DIMUC	U+	Y+
0.500	23.100	21.280	12.800	1.000	1.000	1.417	32.867	307.411
0.400	23.100	21.170	12.490	0.800	0.976	1.383	32.071	245.929
0.300	23.100	20.700	10.900	0.600	0.852	1.207	27.989	184.446
0.200	23.100	20.280	9.600	0.400	0.750	1.063	24.651	122.964
0.150	23.100	19.980	8.950	0.300	0.699	0.991	22.982	92.223
0.100	23.100	19.820	8.700	0.200	0.680	0.963	22.340	61.482
0.050	23.100	19.500	7.900	0.100	0.617	0.875	20.285	30.741
0.020	23.100	18.960	6.700	0.040	0.523	0.742	17.204	12.296

CALIBRATED AVERAGE VELOCITY= 9.030 FRICTION FACTOR= 0.00372000

INTEGRATED AVERAGE VELOCITY= 8.911 REYNOLDS NUMBER= 60932.000

FLOW RATE (POUNDS/MINUTE) = 143.000

MULTI-FILM ANEMOMETER MEASUREMENTS

RUN= 31 POLYISOBUTYLENE (0.4%) IN CYCLOHEXANE

Y	TEM	VOLTAGE	FT/SC	DIMR	DIMU	DIMUC	U+	Y+
0.500	24.100	20.240	16.310	1.000	1.000	1.299	31.216	412.425
0.400	24.100	20.190	15.300	0.800	0.938	1.242	29.283	329.940
0.300	24.100	20.100	14.450	0.600	0.886	1.173	27.656	247.455
0.200	24.100	19.970	13.450	0.400	0.825	1.092	25.743	164.970
0.150	24.100	19.880	12.900	0.300	0.791	1.048	24.690	123.728
0.100	24.100	19.850	12.700	0.200	0.779	1.031	24.307	82.485
0.050	24.100	19.700	11.700	0.100	0.717	0.950	22.393	41.243
0.020	24.100	19.640	11.450	0.040	0.702	0.930	21.915	16.497

CALIBRATED AVERAGE VELOCITY= 12.315 FRICTION FACTOR= 0.00360000

INTEGRATED AVERAGE VELOCITY= 12.568 REYNOLDS NUMBER= 83259.000

FLOW RATE (POINDS/MINUTE) = 195.000

IX NOMENCLATURE

A	constant in equation 11
B	constant in equation 11
b	constant in equation 7
C	constant in equation 12
D	inside diameter of tube
E	voltage
f	friction factor
g_c	gravitational acceleration constant, equal to 32.178 lb-m x ft/lb-f x sec^2
k_k	constant in equation 4
k_p	constant in equation 10
K'	constant in equation 13
$\tilde{l}$	mixing length
L	length between pressure taps
N_{Re}	Reynolds number
$N_{Re(s)}$	Reynolds number of the solvent
n'	constant in equation 13
P	pressure
Q	flow rate
r	radial distance from the center line in a tube
R	inside tube radius
U	average or bulk velocity
$\tilde{u}$	local velocity at some radial position in a tube
u_{max}	center line velocity
u_c	center line velocity

u^+	dimensionless velocity defined by equation 11
u^*	friction velocity
y	radial distance from the pipe wall
y^+	dimensionless distance defined by equation 11
α	constant in equation 16
Δ	difference, as ΔP is difference in pressure
γ	kinematic viscosity
$\mu(t)$	turbulent coefficient of viscosity
μ	viscosity
ρ	density
τ	shear stress
τ_w	shear stress at the wall
σ	normal stress
$\bar{\sigma}_i'$	normal stress, deviatoric component
τ_1	first mode relaxation time

X VITA

Luis Gustavo Florez E., son of Luis B. Florez S. and Josefina Enciso de Florez, was born on May 8, 1941, in Bogota, Colombia.

He attended elementary school in Bogota, Colombia. He graduated from "Externado Nacional Camilo Torres" High School in December 1958. He enrolled in the "Fundacion Universidad de America" in 1959 and received his degree of Chemical Engineer in December 1964. The title of his B.S. thesis is: "Preliminary Design of a Pilot Plant for the Unit Operations Laboratory of the FUA." He served as part time instructor in the Chemistry Department of the "Universidad Distrital" and "Universidad Libre" in Bogota, Colombia, in 1965. In June 1966 he entered the Graduate School of the University of Missouri at Rolla.

XI BIBLIOGRAPHY

1. Astarita, G. and Nicodemo, L., A.I.Ch.E. J., 12, 478 (1966).
2. Bird, R. B., Stewart, W. E., and Lightfoot, E. N., "Transport Phenomena," John Wiley, New York, 1960.
3. Bogue, D. C., Ph.D. thesis, University of Delaware, 1960.
4. Bogue, D. C., and Metzner, A. B., I. & E. C. Fundamentals, 2, 143 (1963).
5. Bunch, D., Ph.D. thesis, University of Missouri at Rolla, 1964.
6. Clapp, R. M., in "International Developments in Heat Transfer, Part III," pp 652-661, ASME, New York, 1961.
7. Deissler, R. G., Trans. ASME, 73, 101 (1957).
8. DISA Electronik, "Operation Manual for Disa Constant Temperature Anemometer," Herlev, Denmark (Aug. 1963).
9. Dodge, D. W., and Metzner, A. B., A.I.Ch.E. J., 5, 189 (1959).
10. Eissenberg, D. M.,A.I.Ch.E. J., 10, 403 (1964).
11. Elata, C., Lehrer, J., and Kahanovitz, A., Israel J. Tech., 4, 84 (1966).
12. Ernst, W. D., A.I.Ch.E. J., 12, 581 (1966).
13. Gill, W. N., and Scher, M., A.I.Ch.E. J., 7, 61 (1961).
14. Goldstein, S., Proc. Roy. Soc., A159, 473 (1937).
15. Hershey, H. C., Ph.D. thesis, University of Missouri at Rolla, 1965.
16. Hershey, H. C., and Zakin, J. L. Ind. Eng. Chem. Fund., 6, 381 (1967).

7. Hinze, J. O., "Turbulence," McGraw Hill, New York (1959).

8. Knudsen, J. G., and Katz, D. L., "Fluid Dynamics and Heat Transfer," McGraw Hill, New York (1958).

9. Lindgren, E. R., and Chao, J. L, Physics of Fluids, 10, 667 (1967).

0. Marrucci, G., and Astarita, G., Ind. Eng. Chem. Fund., 6, 470 (1967).

1. Meter, D. M., Ph.D. thesis, University of Wisconsin, Madison, 1963.

2. Metzner, A. B., and White, J. L., and Denn, M. M., A.I.Ch.E. J., 12, 863 (1966).

3. Metzner, A. B., Houghton, W. T., Sailor, R. A., and White, J. L., Trans. Soc. Rheol., 5, 133 (1961).

. Meyer, W. A., A.I.Ch.E. J., 12, 522 (1966).

. Mooney, M. J., Rheol., 2, 210 (1931).

. Nikuradse, J., N.A.C.A. T.M. 1292 (1950).

. Pai, S. I., "Viscous Flow Theory," Vol. II, Van Nostrand, Princeton (1957).

. Patterson, G. K., Ph.D. thesis, University of Missouri at Rolla, 1966.

, Patterson, G. K., and Zakin, J. L., A.I.Ch.E. J., in press.

Patterson, G. K., Zakin, J. L., and Rodriguez, J. M., unpublished manuscript.

Rabinowitsch, B. Z., Z. Physik. Chem., A145, 1 (1929).

52. Radin, I., M. S. thesis, in progress, University of Missouri at Rolla.

53. Reiner, M., Physics Today, 17, 62, Jan. 1964.

54. Reynolds, O., Trans. Roy. Soc. (London), 174A, 935 (1883).

55. Rodriguez, J. M., M. S. thesis, University of Missouri at Rolla, 1966.

56. Rodriguez, J. M., Zakin, J. L., and Patterson, G. K., Soc. Petr. Eng. J., 7, 325 (1967).

57. Rodriguez, J. M., Ph.D. thesis in progress, University of Missouri at Rolla.

58. Ross, D., N.O.R.D. Report No. 7958246, Penn. St. University, College Park (1952).

59. Savins, J. G., J. Inst. Petr., 47, 329 (1961).

60. Savins, J. G., A.I.Ch.E. J., 11, 673 (1965).

61. Savins, J. G., Soc. Petr. Eng. Jour., 4, 203 (1964).

62. Schlichting, H., "Boundary Layer Theory," McGraw Hill, New York (1955).

63. Shaver, R. G., Sc. D. thesis, M.I.T., 1957.

64. Shaver, R. G., and Merrill, E. W., A.I.Ch.E. J., 5, 181 (1959).

65. Tao, F., Ph.D. thesis, University of Missouri at Rolla, 1964.

66. Toms, B. A., "Proceedings of the (First) International Congress in Rheology," p. II-135, North-Holland Publishing Company, Amsterdam, 1949.

67. Virk, P., Ph.D. thesis, M.I.T., 1966.

8. Wang, C., J. Applied Mechanics, 68, A-85 (1946).

9. Wells, C. S., Jr., A.I.A.A. J., 3, 1800 (1965).